Two Higgs doublet model predictions for $\bar{B}\to X_s\gamma$ in NLO QCD

Francesca M. Borzumati
Institut für Theoretische Physik, Universität Zürich, Winterthurerstrasse 190, 8057 Zürich, Switzerland

Christoph Greub
Institut für Theoretische Physik, Universität Bern, Sidlerstrasse 5, 3012 Bern, Switzerland
(Received 23 February 1998; published 2 September 1998)

The decay $\bar{B}\to X_s\gamma$ is studied at next to leading order in QCD in a class of models containing at least two Higgs doublets and with only one charged Higgs boson nondecoupled at low energy. The two-loop matching condition is calculated and it is found to agree with existing results. The complete dependence of the Wilson coefficients on the matching scale is given. The size of the next to leading order corrections is extensively discussed. Results for branching ratios, possible *CP* asymmetries, and lower bounds on the charged Higgs boson mass are presented when the convergence of the perturbative series appears fast enough to yield reliable predictions. Regions in the parameter space of these models where the next to leading order calculation is still not a good approximation of the final result for these observables are singled out. [S0556-2821(98)07217-8]

PACS number(s): 13.25.Hw, 12.38.Bx

I. INTRODUCTION

It is well known that charged Higgs contributions to the branching ratio for the decay $\bar{B}\to X_s\gamma$, $B(\bar{B}\to X_s\gamma)$, decouple very slowly from the standard model (SM) one. Hence, in the absence of any experimental evidence for a charged Higgs boson, this decay may provide a powerful tool to limit the range of unknown parameters in models where such a particle is present and other, nonstandard, contributions to $B(\bar{B}\to X_s\gamma)$ are subleading [1,2].

Supersymmetric models constitute, perhaps, the best motivated extension of the SM where a second Higgs doublet, and therefore a charged Higgs boson $H^\pm$, is necessary for internal consistency [3]. Simpler extensions where only Higgs doublets are added to the SM are, however, important on their own right. They are also excellent pedagogical tools to understand the subtleties that the next to leading order (NLO) calculation of $B(\bar{B}\to X_s\gamma)$ entails, and which may be hidden in the SM results.

The simplest class of such extensions, with two Higgs doublets, is usually denoted as 2HDMs. This class contains the well-known type-I and type-II models in which the same or the two different Higgs fields couple to up- and down-type quarks. For what concerns us here, multi-Higgs-doublet models can be included in this class, provided only one charged Higgs boson remains light enough to be relevant for the process $\bar{B}\to X_s\gamma$. This generalization allows a simultaneous study of $\bar{B}\to X_s\gamma$ in different models, including type I and type II, by a continuous variation of the (generally complex) charged Higgs couplings to fermions. (No tree-level flavor violating neutral couplings are assumed in the present paper.) It also allows a more complete investigation of the question whether the measurement of $B(\bar{B}\to X_s\gamma)$ closes the possibility of a relatively light $H^\pm$ not embedded in a supersymmetric model [4].

At present, a measurement of this decay rate by the CLEO Collaboration is available [5]:

$$B(\bar{B}\to X_s\gamma)=(2.32\pm 0.57\pm 0.35)\times 10^{-4}. \tag{1}$$

There also exists a preliminary result by the ALEPH Collaboration with a larger central value [6]:

$$B(\bar{B}\to X_s\gamma)=(3.11\pm 0.80\pm 0.72)\times 10^{-4}. \tag{2}$$

Adding statistical and systematical errors in quadrature, one obtains 90% C.L. lower and upper limits on $B(\bar{B}\to X_s\gamma)$ of 1.22×10^{-4} and 3.42×10^{-4} from the CLEO measurement and 1.34×10^{-4}, 4.88×10^{-4} from the ALEPH result. The band of allowed values, corresponding to a more conservative estimate of the systematic error, is reported by CLEO to be $(1.0-4.2)\times 10^{-4}$ [5].

The theoretical situation within the SM, is at the moment far better settled than the experimental one. After the original observation that QCD corrections to the decay $\bar{B}\to X_s\gamma$ are a substantial fraction of its rate [7], a collective theoretical effort of almost a decade has led to the determination of $B(\bar{B}\to X_s\gamma)$ at the NLO in QCD, and to a considerable reduction of the theoretical error. For the leading order (LO) calculation, several groups contributed to the evaluation of the elements of the anomalous dimension matrix [8,9] and provided phenomenological analyses with partial inclusion of some NLO contributions (e.g., bremsstrahlung corrections) [10–13]. The two-loop matching condition, needed for a complete NLO calculation, was first obtained in Ref. [14] and later confirmed in Refs. [15–17], using different techniques. The two-loop corrections to the matrix elements were calculated [18] and the determination of the $\mathcal{O}(\alpha_s^2)$ elements of the anomalous dimension matrix, started already since some time [19,20], has been completed only recently [21,22]. In addition, nonperturbative contributions to $B(\bar{B}\to X_s\gamma)$, scaling as $1/m_b^2$ [23–25] and $1/m_c^2$ [26], were also computed. The issue of the dependence of the branching ratio on scales, first raised at the LO level in Refs. [11,13], was addressed for the NLO calculation, and discussed in detail, in Ref. [27]. In the SM, uncertainties due to sensitivity of

$B(\overline{B}\to X_s\gamma)$ on such scales are small and the theoretical estimate for this observable suffers mainly from the large experimental errors of the input parameters.

It would be desirable to have similarly precise calculations also in extensions of the SM. Thus, more accurate experimental measurements, when available, could provide stringent constraints on the free parameters of these models. We present here a detailed study of $B\to X_s\gamma$ at the NLO in QCD, in the class of models specified above, aiming, in particular, to obtain an assessment of the reliability of the theoretical calculation. Our results are, in general, less optimistic than one could have foreseen. Indeed, we find unexpectedly large NLO corrections and scale dependences in the Higgs contributions to $B(\overline{B}\to X_s\gamma)$, irrespective of the value of the charged Higgs couplings to fermions. This feature remains undetected in type-II models, where the SM contribution to $B(\overline{B}\to X_s\gamma)$ is always larger than, and in phase with, the Higgs contributions. It can, however, produce unacceptably large scale uncertainties for certain ranges of these couplings and, at times, completely ill-defined results which are expected to be cured by even higher order QCD corrections. We single out combinations of couplings and of values of the charged Higgs mass m_H for which the branching ratio can be reliably predicted at this order in QCD. In this case, a comparison between theoretical and experimental results for $B(\overline{B}\to X_s\gamma)$ allows us to conclude that values of $m_H=\mathcal{O}(M_W)$ can be excluded, in general, only in type-II models, but are otherwise allowed.

Previous LO analyses dealt with type-I and type-II models [8,28–30] and the generalized class of models considered here [31,32]. LO calculations are known to have large scale uncertainties. Consequently, they are not particularly good arenas to distinguish the quantitative differences between QCD corrections to charged Higgs and SM contributions. These differences stand out clearly at the NLO level. Two NLO calculations have been performed recently [17,33]. They deal with type-I and type-II models and the issue of scale uncertainty is addressed in Ref. [17] for type-II models. The fact that the NLO corrections to the Higgs contributions are large is, therefore, understandably missed, since the branching ratio is dominated by the SM contribution. From the technical point of view, our calculation of the two-loop matching condition agrees with that reported in Refs. [17,33]. The analytic dependence of $B(\overline{B}\to X_s\gamma)$ on the matching scale is also in agreement with the published results, after having been corrected in Refs. [27,17].

The remainder of this paper is organized as follows. In Sec. II we define the class of two Higgs doublet models (2HDMs) studied. In Sec. III we outline the main steps of the calculation; to keep this section readable, we relegate some parts of our results to appendixes. In Sec. IV we present our phenomenological analysis of the decay $\overline{B}\to X_s\gamma$ in the class of models considered. After giving our branching ratio prediction for the SM, we discuss, in Sec. IV A, the size of the NLO corrections to the charged Higgs contributions at the amplitude level. In Sec. IV B, we give results for $B(\overline{B}\to X_s\gamma)$ for various ranges of real couplings of the charged Higgs boson to fermions. We discuss their reliability and point to the technical reason for the possible appearance of large scale instabilities. NLO branching ratios for type-I and type-II models are in particular studied in Sec. IV C, where lower bounds for m_H, are given within type-II models. In Sec. IV D, we consider the decay $\overline{B}\to X_s\gamma$ when complex couplings are involved and we investigate the impact of their phases on *CP* rate asymmetries of $\overline{B}\to X_s\gamma$. We also give specific examples of couplings for which the theoretical prediction of the branching ratio is reliable and compatible with the CLEO measurement, even for $m_H=\mathcal{O}(M_W)$. Finally, our concluding remarks are in Sec. V.

II. TWO HIGGS DOUBLET MODELS

Models with more than one Higgs doublet have generically a Yukawa Lagrangian of the form

$$-\mathcal{L}=h^d_{ij}\overline{q'_{Li}}\phi_1 d'_{Rj}+h^u_{ij}\overline{q'_{Li}}\tilde{\phi}_2 u'_{Rj}+h^l_{ij}\overline{l'_{Li}}\phi_3 e'_{Rj}+\text{H.c.}, \tag{3}$$

where q'_L, l'_L, ϕ_i, $(i=1,2,3)$ are SU(2) doublets ($\tilde{\phi}_i=i\sigma^2\phi_i^*$), u'_R, d'_R, and e'_R are SU(2) singlets, and h^d, h^u, and h^l denote 3×3 Yukawa matrices. Gauge invariance imposes the value of hypercharge $Y(\phi_i)=\frac{1}{2}$. Suitable discrete symmetries are usually invoked to forbid additional terms such as $h^d_{ij}\overline{q'_{Li}}\phi_2 d'_{Rj}$ which would induce flavor changing neutral couplings at the tree level. Indeed, to avoid them altogether, it is sufficient to impose that no more than one Higgs doublet couples to the same right-handed field [34].

When only two Higgs doublets are present, ϕ_1 and ϕ_2, it is in general $\phi_3=\phi_1$ (or $\phi_3=\phi_2$). Nevertheless, for the sake of generality, we leave the symbol ϕ_3 distinct from the other two. We indeed also include in our discussion, as ''effective'' 2HDMs, models where an n number of sequential Higgs doublets is present and we assume that the additional charged Higgs bosons other than the lightest one become heavy enough to decouple from our problem.

After rotating the fermion fields from the current eigenstate to the mass eigenstate basis, the charged Higgs component in Eq. (3) becomes

$$-\mathcal{L}=\frac{m_{di}}{\langle\phi_1^0\rangle}\overline{u}_{Lj}V_{ji}d_{Ri}\phi_1^+-\frac{m_{ui}}{\langle\phi_2^0\rangle}\overline{u}_{Ri}V_{ij}d_{Lj}\phi_2^+ +\frac{m_{li}}{\langle\phi_3^0\rangle}\overline{\nu}_{Li}e_{Ri}\phi_3^++\text{H.c.}, \tag{4}$$

where V_{ji} are elements of the Cabibbo-Kobayashi-Maskawa (CKM) matrix. A further rotation of the charged Higgs fields to their physical basis through a unitary matrix U

$$\begin{pmatrix}\phi_1^+\\ \phi_2^+\\ \phi_3^+\\ \cdots\\ \phi_n^+\end{pmatrix}=U\begin{pmatrix}\phi^+\\ H^+\\ \mathcal{H}_1^+\\ \cdots\\ \mathcal{H}_{n-2}^+\end{pmatrix} \tag{5}$$

yields the following Yukawa interaction for H^+:

$$\mathcal{L}=\frac{g}{\sqrt{2}}\left\{\left(\frac{m_{di}}{M_W}\right)X\overline{u}_{Lj}V_{ji}d_{Ri}+\left(\frac{m_{ui}}{M_W}\right)Y\overline{u}_{Ri}V_{ij}d_{Lj}+\left(\frac{m_{li}}{M_W}\right)Z\overline{\nu}_{Li}e_{Ri}\right\}H^+ + \text{H.c.} \tag{6}$$

All fields $\mathcal{H}_i^+$ are supposed to be heavy enough to become irrelevant for phenomenology at the electroweak scale. In Eq. (6), the symbols X and Y are defined in terms of elements of the matrix U [35–37,31,32]:

$$X=-\frac{U_{12}}{U_{11}},\quad Y=\frac{U_{22}}{U_{21}}. \tag{7}$$

The symbol Z has a similar definition, i.e., $Z=-U_{32}/U_{31}$ if $\phi_3\neq\phi_1,\phi_2$ or coincides with $X(-Y)$ if $\phi_3=\phi_1$ $(\phi_3=\phi_2)$. Notice that X, Y, and Z are in general complex numbers and therefore potential sources of CP violating effects [38,39]. Their values are only very loosely constrained by the requirement of perturbativity and low-energy processes such as the B-$\overline{B}$ mixing [32].

When only two doublets are considered, the diagonalization matrix U is a 2×2 orthogonal matrix

$$\begin{pmatrix}\cos\beta & -\sin\beta\\ \sin\beta & \cos\beta\end{pmatrix}. \tag{8}$$

Although both doublets are present in the theory, one still has the freedom of selecting $\phi_1=\phi_2$ in Eq. (3). This choice gives rise to the 2HDM of type I, to be distinguished from the type II in which both doublets contribute to the Yukawa interactions [40]. It is easy to see that in these two cases the couplings X and Y are real and given by

$$\begin{aligned}&X=-\cot\beta,\quad Y=\cot\beta\quad(\text{type I}),\\ &X=\tan\beta,\quad Y=\cot\beta\quad(\text{type II}).\end{aligned} \tag{9}$$

Note that the coupling of the Goldstone boson ϕ^+ to matter fields is independent of the number n of Higgs doublets considered, and always equal to

$$\mathcal{L}=\frac{-g}{\sqrt{2}}\left\{\left(\frac{m_{di}}{M_W}\right)\overline{u}_{Lj}V_{ji}d_{Ri}-\left(\frac{m_{ui}}{M_W}\right)\overline{u}_{Ri}V_{ij}d_{Lj}+\left(\frac{m_{li}}{M_W}\right)\overline{\nu}_{Li}e_{Ri}\right\}\phi^+ + \text{H.c.} \tag{10}$$

The calculation of the $\overline{B}\to X_s\gamma$ decay rate in these models, therefore, is modified simply by the addition of charged Higgs contributions to the usual SM one. The results can be described in terms of m_H and the two complex parameters X and Y. The presence of phases in the couplings X and Y allows for CP asymmetries in the decay rate for $B\to X_s\gamma$.

III. THE CALCULATION

We use the framework of an effective low-energy theory with five quarks, obtained by integrating out the heavy degrees of freedom, which in the present case are the t quark, the W boson, and the charged Higgs boson. As in the SM calculations, we only take into account operators up to dimension 6 and we put $m_s=0$. In this approximation the effective Hamiltonian relevant for radiative B decays (with $|\Delta B|=|\Delta S|=1$),

$$\mathcal{H}_{\text{eff}}=-\frac{4G_F}{\sqrt{2}}V_{ts}^{\star}V_{tb}\sum_{i=1}^{8}C_i(\mu)\mathcal{O}_i(\mu), \tag{11}$$

consists precisely of the same operators $\mathcal{O}_i(\mu)$ used in the SM case, weighted by the Wilson coefficients $C_i(\mu)$. They read

$$\begin{aligned}
\mathcal{O}_1&=(\overline{s}_L\gamma_\mu T^a c_L)(\overline{c}_L\gamma^\mu T_a b_L),\\
\mathcal{O}_2&=(\overline{s}_L\gamma_\mu c_L)(\overline{c}_L\gamma^\mu b_L),\\
\mathcal{O}_3&=(\overline{s}_L\gamma_\mu b_L)\sum_q(\overline{q}\gamma^\mu q),\\
\mathcal{O}_4&=(\overline{s}_L\gamma_\mu T^a b_L)\sum_q(\overline{q}\gamma^\mu T_a q),\\
\mathcal{O}_5&=(\overline{s}_L\gamma_\mu\gamma_\nu\gamma_\rho b_L)\sum_q(\overline{q}\gamma^\mu\gamma^\nu\gamma^\rho q),\\
\mathcal{O}_6&=(\overline{s}_L\gamma_\mu\gamma_\nu\gamma_\rho T^a b_L)\sum_q(\overline{q}\gamma^\mu\gamma^\nu\gamma^\rho T_a q),\\
\mathcal{O}_7&=\frac{e}{16\pi^2}\overline{m}_b(\mu)(\overline{s}_L\sigma^{\mu\nu}b_R)F_{\mu\nu},\\
\mathcal{O}_8&=\frac{g_s}{16\pi^2}\overline{m}_b(\mu)(\overline{s}_L\sigma^{\mu\nu}T^a b_R)G^a_{\mu\nu},
\end{aligned} \tag{12}$$

where T^a $(a=1,8)$ are SU(3) color generators and g_s and e are the strong and electromagnetic coupling constants. In Eq. (12), $\overline{m}_b(\mu)$ is the running b-quark mass in the modified minimal subtraction ($\overline{\text{MS}}$) scheme at the renormalization scale μ. Henceforth, $\overline{m}_q(\mu)$ and m_q denote $\overline{\text{MS}}$ running and pole masses, respectively. To first order in α_S, these masses are related through

$$\overline{m}_q(\mu)=m_q\left(1+\frac{\alpha_S(\mu)}{\pi}\ln\frac{m_q^2}{\mu^2}-\frac{4}{3}\frac{\alpha_S(\mu)}{\pi}\right). \tag{13}$$

Note that the equations of motion have been used when writing down the list of operators in Eq. (12). This is sufficient since we are interested in on-shell matrix elements [41] and since we choose to perform the matching by comparing on-shell amplitudes obtained in the effective theory with the corresponding amplitudes in the full theory. The reader who is interested in doing off-shell matching [and therefore working in a (larger) off-shell operator basis] is referred to Ref. [17].

Working to NLO precision means that one is resumming all the terms of the form $\alpha_S^n(m_b)\ln^n(m_b/M)$, as well as $\alpha_S(m_b)$ $[\alpha_S^n(m_b)\ln^n(m_b/M)]$, where M stands for one of the heavy masses M_W, m_t, or m_H. This is achieved by performing the following three steps.

(1) One matches the full standard model theory with the effective theory at a scale μ_W, of order M. At this scale, the matrix elements of the operators in the effective theory lead to the same logarithms as the calculation in the full theory. Consequently, the Wilson coefficients $C_i(\mu_W)$ only pick up ''small'' QCD corrections, which can be calculated in fixed order perturbation theory. In the NLO program, the matching has to be worked out at the $O(\alpha_S)$ level.

(2) The evolution of these Wilson coefficients from $\mu=\mu_W$ down to $\mu=\mu_b$, where μ_b is of the order of m_b, is obtained by solving the appropriate renormalization group equation (RGE). As the matrix elements of the operators evaluated at the low scale μ_b are free of large logarithms, the latter are contained in resummed form in the Wilson coefficients. For a NLO calculation, this step has to be performed using the anomalous dimension matrix up to order α_S^2.

(3) The corrections to the matrix elements of the operators $\langle s\gamma|\mathcal{O}_i(\mu)|b\rangle$ at the scale $\mu=\mu_b$ have to be calculated to order α_S precision.

The charged Higgs boson enters the NLO calculation only via step (1). The Higgs boson contribution to the matching condition is obtained in the same way as the SM one [15]; therefore, we do not repeat any technical details. A general remark, however, is in order. In the procedure described above all heavy particles (W boson, t quark, and charged Higgs boson) are integrated out simultaneously at the scale μ_W. In the context of a NLO calculation this should be a reasonable approximation provided m_H is of the same order of magnitude as M_W or m_t.

Before giving the results of the three steps listed above, we should briefly mention that instead of the original Wilson coefficients $C_i(\mu)$ it is convenient to use certain linear combinations of them, the so-called ''effective Wilson'' coefficients $C_i^{\rm eff}(\mu)$ introduced in Refs. [13,21]

$$C_i^{\rm eff}(\mu)=C_i(\mu)\quad (i=1,\ldots,6),$$

$$C_7^{\rm eff}(\mu)=C_7(\mu)+\sum_{i=1}^{6} y_i C_i(\mu),$$

$$C_8^{\rm eff}(\mu)=C_8(\mu)+\sum_{i=1}^{6} z_i C_i(\mu), \tag{14}$$

where y_i and z_i are defined in such a way that the leading order matrix elements $\langle s\gamma|\mathcal{O}_i|b\rangle$ and $\langle sg|\mathcal{O}_i|b\rangle$ $(i=1,6)$ are absorbed in the leading orders terms in $C_7^{\rm eff}(\mu)$ and $C_8^{\rm eff}(\mu)$. The explicit values of $\{y_i\}$ and $\{z_i\}$, $y=(0,0,-\frac{1}{3},-\frac{4}{9},-\frac{20}{3},-\frac{80}{9})$, $z=(0,0,1,-\frac{1}{6},20,-\frac{10}{3})$ were obtained in Ref. [21] in the $\overline{\rm MS}$ scheme with fully anticommuting γ_5 (also used in the present paper).

A. NLO Wilson coefficients at the matching scale μ_W: $C_i^{\rm eff}(\mu_W)$

To give the results for the effective Wilson coefficients $C_i^{\rm eff}$ at the matching scale μ_W in a compact form, we write

$$C_i^{\rm eff}(\mu_W)=C_i^{0,\rm eff}(\mu_W)+\frac{\alpha_S(\mu_W)}{4\pi}\,C_i^{1,\rm eff}(\mu_W). \tag{15}$$

The LO Wilson coefficients at this scale are well known [42,28]. We decompose them in such a way to render explicit their dependence on the couplings X and Y:

$$\begin{aligned}
&C_2^{0,\rm eff}(\mu_W)=1,\\
&C_i^{0,\rm eff}(\mu_W)=0\quad (i=1,3,4,5,6),\\
&C_7^{0,\rm eff}(\mu_W)=C_{7,\rm SM}^0+|Y|^2C_{7,YY}^0+(XY^*)C_{7,XY}^0,\\
&C_8^{0,\rm eff}(\mu_W)=C_{8,\rm SM}^0+|Y|^2C_{8,YY}^0+(XY^*)C_{8,XY}^0.
\end{aligned} \tag{16}$$

The coefficients $C_{7,\rm SM}^0(\mu_W)$ and $C_{8,\rm SM}^0(\mu_W)$ are functions of $x=m_t^2/M_W^2$, while $C_{7,j}^0(\mu_W)$ and $C_{8,j}^0(\mu_W)$ $(j=YY,XY)$ are functions of $y=m_t^2/m_H^2$; their explicit forms are given in Appendix A. Note that there is no *explicit* dependence of the matching scale μ_W in these functions. Whether there is an implicit μ_W dependence via the t-quark mass depends on the precise definition of this mass which has to be specified when going beyond leading logarithms. If one chooses, for example, to work with $\overline{m_t}(\mu_W)$, then there is such an implicit μ_W dependence of the lowest order Wilson coefficient; in contrast, when working with the pole mass m_t there is no such dependence. We choose to express our (NLO) results in terms of the pole mass m_t.

The NLO pieces $C_i^{1,\rm eff}(\mu_W)$ of the Wilson coefficients have an explicit dependence on the matching scale μ_W and for $i=7,8$ they also explicitly depend on the actual definition of the t-quark mass. Initially, when the heavy particles are integrated out, it is convenient to work out the matching conditions $C_i^{1,\rm eff}(\mu_W)$ for $i=7,8$ in terms of $\overline{m_t}(\mu_W)$. Using Eq. (13), it is then straightforward to get the corresponding result expressed in terms of the pole mass m_t. As in the LO case we give them in a form where the dependence of the couplings X and Y is explicit:

$$\begin{aligned}
&C_1^{1,\rm eff}(\mu_W)=15+6\ln\frac{\mu_W^2}{M_W^2},\\
&C_4^{1,\rm eff}(\mu_W)=E_0+\frac{2}{3}\ln\frac{\mu_W^2}{M_W^2}+|Y|^2E_H,\\
&C_i^{1,\rm eff}(\mu_W)=0\quad (i=2,3,5,6),\\
&C_7^{1,\rm eff}(\mu_W)=C_{7,\rm SM}^{1,\rm eff}(\mu_W)+|Y|^2C_{7,YY}^{1,\rm eff}(\mu_W)\\
&\qquad\qquad +(XY^*)C_{7,XY}^{1,\rm eff}(\mu_W),
\end{aligned}$$

$$C_8^{1,\mathrm{eff}}(\mu_W)=C_{8,\mathrm{SM}}^{1,\mathrm{eff}}(\mu_W)+|Y|^2C_{8,YY}^{1,\mathrm{eff}}(\mu_W)+(XY^*)C_{8,XY}^{1,\mathrm{eff}}(\mu_W), \tag{17}$$

where for $i=7,8$ the three terms on the right-hand side can be written in the form

$$C_{i,\mathrm{SM}}^{1,\mathrm{eff}}(\mu_W)=W_{i,\mathrm{SM}}+M_{i,\mathrm{SM}}\ln\frac{\mu_W^2}{M_W^2}+T_{i,\mathrm{SM}}\left(\ln\frac{m_t^2}{\mu_W^2}-\frac{4}{3}\right),$$

$$C_{i,YY}^{1,\mathrm{eff}}(\mu_W)=W_{i,YY}+M_{i,YY}\ln\frac{\mu_W^2}{m_H^2}+T_{i,YY}\left(\ln\frac{m_t^2}{\mu_W^2}-\frac{4}{3}\right),$$

$$C_{i,XY}^{1,\mathrm{eff}}(\mu_W)=W_{i,XY}+M_{i,XY}\ln\frac{\mu_W^2}{m_H^2}+T_{i,XY}\left(\ln\frac{m_t^2}{\mu_W^2}-\frac{4}{3}\right). \tag{18}$$

Note that in Eq. (18) the $W_{i,j}$ and the $M_{i,j}$ ($j=\mathrm{SM},XY,YY$) terms would be the full result when working in terms of $\overline{m}_t(\mu_W)$. The $T_{i,j}$ terms result when expressing $\overline{m}_t(\mu_W)$ in terms of the pole mass m_t in the corresponding lowest order coefficients. Thus, for $i=7,8$, the $T_{i,j}$ quantities are

$$T_{i,\mathrm{SM}}=8x\,\frac{\partial C_{i,\mathrm{SM}}^{0,\mathrm{eff}}(\mu_W)}{\partial x},$$

$$T_{i,j}=8y\,\frac{\partial C_{i,j}^{0,\mathrm{eff}}(\mu_W)}{\partial y}\quad(j=XY,YY). \tag{19}$$

Notice that if one worked with the running t-quark mass $\overline{m}_t(\mu_t)$ normalized at the scale μ_t instead of the pole mass m_t, the third terms on the right-hand sides of Eqs. (18) would have to be replaced by $T_{i,j}\ln(\mu_t^2/\mu_W^2)$ ($j=\mathrm{SM},YY,XY$). The functions $W_{i,j}$, $M_{i,j}$, and $T_{i,j}$ ($j=\mathrm{SM},XY,YY$), together with E_0 and E_H, are listed in Appendix A. Our results for $C_7^{1,\mathrm{eff}}(\mu_W)$ and $C_8^{1,\mathrm{eff}}(\mu_W)$ agree with those in Refs. [33] and [17], when taking into account that the latter results are expressed in terms of $\overline{m}_t(\mu_W)$. As correct is also recognized the form of $C_1^{1,\mathrm{eff}}(\mu_W)$ and $C_4^{1,\mathrm{eff}}(\mu_W)$ in the final version of Refs. [27,17].

B. NLO Wilson coefficients at the low-scale μ_b: $C_i^{\mathrm{eff}}(\mu_b)$

The evolution from the matching scale μ_W down to the low-energy scale μ_b is described by the RGE

$$\mu\,\frac{d}{d\mu}\,C_i^{\mathrm{eff}}(\mu)=C_j^{\mathrm{eff}}(\mu)\,\gamma_{ji}^{\mathrm{eff}}(\mu). \tag{20}$$

The initial conditions $C_i^{\mathrm{eff}}(\mu_W)$ for this equation are given in Sec. III A, and the anomalous dimension matrix $\gamma_{ij}^{\mathrm{eff}}$ is given in Appendix B up to order α_S^2, which is the precision needed for a NLO calculation. The solution of Eq. (20), obtained through the procedure described in Ref. [43], yields for the coefficient

$$C_i^{\mathrm{eff}}(\mu_b)=C_i^{0,\mathrm{eff}}(\mu_b)+\frac{\alpha_S(\mu_b)}{4\pi}\,C_i^{1,\mathrm{eff}}(\mu_b), \tag{21}$$

the LO term

$$C_7^{0,\mathrm{eff}}(\mu_b)=\eta^{16/23}C_7^{0,\mathrm{eff}}(\mu_W)+\frac{8}{3}\,(\eta^{14/23}-\eta^{16/23})C_8^{0,\mathrm{eff}}(\mu_W)+\sum_{i=1}^{8}h_i\,\eta^{\alpha_i}C_2^{0,\mathrm{eff}}(\mu_W) \tag{22}$$

and the NLO term

$$\begin{aligned}C_7^{1,\mathrm{eff}}(\mu_b)=&\,\eta^{39/23}C_7^{1,\mathrm{eff}}(\mu_W)+\frac{8}{3}\,(\eta^{37/23}-\eta^{39/23})C_8^{1,\mathrm{eff}}(\mu_W)\\&+\left(\frac{297\,664}{14\,283}\,\eta^{16/23}-\frac{7\,164\,416}{357\,075}\,\eta^{14/23}\right.\\&\left.+\frac{256\,868}{14283}\,\eta^{37/23}-\frac{6\,698\,884}{357075}\,\eta^{39/23}\right)C_8^{0,\mathrm{eff}}(\mu_W)\\&+\frac{37\,208}{4761}\,(\eta^{39/23}-\eta^{16/23})C_7^{0,\mathrm{eff}}(\mu_W)\\&+\sum_{i=1}^{8}[e_i\,\eta C_4^{1,\mathrm{eff}}(\mu_W)+(f_i+k_i\,\eta)C_2^{0,\mathrm{eff}}(\mu_W)\\&+l_i\,\eta C_1^{1,\mathrm{eff}}(\mu_W)]\,\eta^{a_i}.\end{aligned} \tag{23}$$

The symbol η is defined as $\eta=\alpha_s(\mu_W)/\alpha_S(\mu_b)$; the vectors a_i, h_i, e_i, f_i, k_i, and l_i are listed in Appendix C. Notice that Eq. (23) can be used in this form for all models in which the same set of coefficients $C_i(\mu_W)$ are nonvanishing. It is more general than the corresponding Eq. (21) given in Ref. [21], which can be used only when the matching scale μ_W is fixed at the value M_W.

As far as the other Wilson coefficients are concerned, they are only needed to LO precision in the complete NLO analysis of $B(\overline{B}\to X_s\gamma)$. In this precision, the Wilson coefficients of the four-Fermi operators ($i=1,\ldots,6$) are the same as in the SM. As the coefficients $C_3^{\mathrm{eff}}(\mu_b),\ldots,C_6^{\mathrm{eff}}(\mu_b)$ are numerically much smaller than $C_2^{\mathrm{eff}}(\mu_b)$, we neglect contributions proportional to these small Wilson coefficients in the amplitude for $B(\overline{B}\to X_s\gamma)$ and list here only the LO expressions for $C_1^{\mathrm{eff}}(\mu_b)$, $C_2^{\mathrm{eff}}(\mu_b)$, and $C_8^{\mathrm{eff}}(\mu_b)$:

$$\begin{aligned}C_1^{0,\mathrm{eff}}(\mu_b)=&\,(\eta^{6/23}-\eta^{-12/23})C_2^{0,\mathrm{eff}}(\mu_W),\\C_2^{0,\mathrm{eff}}(\mu_b)=&\left(\frac{2}{3}\,\eta^{6/23}+\frac{1}{3}\,\eta^{-12/23}\right)C_2^{0,\mathrm{eff}}(\mu_W),\\C_8^{0,\mathrm{eff}}(\mu_b)=&\,\eta^{14/23}C_8^{0,\mathrm{eff}}(\mu_W)\\&+\sum_{i=1}^{5}h_i'\,\eta^{a_i'}C_2^{0,\mathrm{eff}}(\mu_W).\end{aligned} \tag{24}$$

When discussing the contributions due to the charged Higgs boson, it is convenient to split the Wilson coefficients at the scale μ_b into the contributions $C_{i,\mathrm{SM}}^{\mathrm{eff}}(\mu_b)$, $C_{i,YY}^{\mathrm{eff}}(\mu_b)$, and $C_{i,XY}^{\mathrm{eff}}(\mu_b)$:

$$C_i^{\mathrm{eff}}(\mu_b)=C_{i,\mathrm{SM}}^{\mathrm{eff}}(\mu_b)+|Y|^2C_{i,YY}^{\mathrm{eff}}(\mu_b)+(XY^*)C_{i,XY}^{\mathrm{eff}}(\mu_b). \tag{25}$$

As the solution (23) of the renormalization group equation (20) is linear in the initial conditions, this splitting is given in an obvious way in terms of the corresponding splitting at the matching scale μ_W, presented in Sec. III A.

When calculating NLO results in the numerical analyses in Sec. IV, we use the NLO expression for the strong coupling constant

$$\alpha_S(\mu)=\frac{\alpha_S(M_Z)}{v(\mu)}\left[1-\frac{\beta_1}{\beta_0}\frac{\alpha_S(M_Z)}{4\pi}\frac{\ln v(\mu)}{v(\mu)}\right] \tag{26}$$

with

$$v(\mu)=1-\beta_0\frac{\alpha_S(M_Z)}{2\pi}\ln\left(\frac{M_Z}{\mu}\right), \tag{27}$$

where $\beta_0=\frac{23}{3}$ and $\beta_1=\frac{116}{3}$. However, for LO results we always use the LO expression for $\alpha_S(\mu)$, i.e., β_1 is put to zero in Eq. (26).

C. Branching ratio for $B(\bar{B}\to X_s\gamma)$

We first give the formulas for the quark decay $b\to X_s\gamma$ and discuss the meson decay $\bar{B}\to X_s\gamma$ later. In a NLO calculation, $b\to X_s\gamma$ involves the subprocesses $b\to s\gamma$ (including virtual corrections) and $b\to s\gamma g$, i.e., the gluon bremsstrahlung process. The amplitude for the first can be written as

$$\mathcal{A}(b\to s\gamma)=-\frac{4G_F}{\sqrt{2}}V_{ts}^{\star}V_{tb}\bar{D}\langle s\gamma|\mathcal{O}_7|b\rangle_{\mathrm{tree}}, \tag{28}$$

where the reduced amplitude $\bar{D}$ is

$$\bar{D}=C_7^{0,\mathrm{eff}}(\mu_b)+\frac{\alpha_S(\mu_b)}{4\pi}[C_7^{1,\mathrm{eff}}(\mu_b)+V(\mu_b)]. \tag{29}$$

The symbol $V(\mu_b)$ is defined as

$$V(\mu_b)=\sum_{i=1}^{8}C_i^{0,\mathrm{eff}}(\mu_b)\left[r_i+\frac{1}{2}\gamma_{i7}^{0,\mathrm{eff}}\ln\frac{m_b^2}{\mu_b^2}\right]-\frac{16}{3}C_7^{0,\mathrm{eff}}(\mu_b). \tag{30}$$

In writing Eq. (28) we directly converted the running mass factor $\overline{m_b}(\mu_b)$, which appears in the definition of the operator $\mathcal{O}_7$ in Eq. (12), into the pole mass m_b by making use of Eq. (13). This conversion is absorbed into the function $V(\mu_b)$ and consequently the symbol $\langle s\gamma|\mathcal{O}_7|b\rangle_{\mathrm{tree}}$ is the tree-level matrix element of the operator $\mathcal{O}_7$, where the running mass factor $\overline{m_b}(\mu_b)$ is understood to be replaced by the pole mass m_b. In the previous literature, this procedure was done in two steps. First, $\overline{m_b}(\mu_b)$ was expressed in terms of $\overline{m_b}(m_b)$ and then in turn $\overline{m_b}(m_b)$ was converted into the pole mass m_b. This last step brought into the game the quantity F (see, e.g., Ref. [18]). The elements $\gamma_{i7}^{0,\mathrm{eff}}$ of the anomalous dimension matrix and the virtual correction functions r_i in Eq. (30) are given in Appendixes B and D, respectively. Note, that some parts of the bremsstrahlung contributions associated with $\mathcal{O}_7$ are effectively transferred to r_7 as detailed in Ref. [18].

A splitting analogous to that in Eq. (25) holds also for the reduced amplitude $\bar{D}$,

$$\bar{D}=\bar{D}_{\mathrm{SM}}+|Y|^2\bar{D}_{YY}+(XY^*)\bar{D}_{XY}, \tag{31}$$

as well as for the function $V(\mu_b)$.

From $\mathcal{A}(b\to s\gamma)$ in Eq. (28) the decay width $\Gamma(b\to s\gamma)$ is easily obtained to be

$$\Gamma(b\to s\gamma)=\frac{G_F^2}{32\pi^4}|V_{ts}^{\star}V_{tb}|^2\alpha_{em}m_b^5|\bar{D}|^2. \tag{32}$$

In the numerics we discard those terms in $|\bar{D}|^2$ which are explicitly of order α_S^2. Note, however, that there are implicit higher order terms which are retained. Such terms arise for example because we evaluate the quantity $\eta=[\alpha_S(\mu_W)/\alpha_S(\mu_b)]$ using the NLO expression for α_S also in those Wilson coefficients which are needed only in LO precision.

To obtain the inclusive rate for $b\to X_s\gamma$ consistently at the NLO level, we have to take into account the bremsstrahlung contributions [10,44]. The corresponding decay width $\Gamma(b\to s\gamma g)$ is of the form

$$\Gamma(b\to s\gamma g)=\frac{G_F^2}{32\pi^4}|V_{ts}^{\star}V_{tb}|^2\alpha_{em}m_b^5A, \tag{33}$$

where A is

$$A=\frac{\alpha_S(\mu_b)}{\pi}\sum_{i,j=1;i\leqslant j}^{8}\mathrm{Re}\{C_i^{0,\mathrm{eff}}(\mu_b)[C_j^{0,\mathrm{eff}}(\mu_b)]^*f_{ij}\}. \tag{34}$$

As in the virtual contributions we put $C_i^{0,\mathrm{eff}}=0$ for $i=3,\ldots,6$. In contrast to Ref. [21], we do not introduce a cutoff when the photon gets soft. In order to cancel the infrared singularity, which appears in this case, we include as in Ref. [18] the virtual photonic correction to the process $b\to sg$, which we absorb into the quantity f_{88} (see Eq. (B9) in Ref. [18]). Note also that in our approach the term f_{77} is already absorbed into the function r_7. The nonvanishing f_{ij} terms, which have to be taken into account explicitly in Eq. (34), are listed in Appendix E.

In order to get the decay width for the meson decay $\bar{B}\to X_s\gamma$ we take into account the nonperturbative corrections which scale as $1/m_b^2$ [23] and those which scale as $1/m_c^2$ [26]. The decay width $\Gamma(B\to X_s\gamma)$ then reads

$$\Gamma(\bar{B}\to X_s\gamma)=\frac{G_F^2}{32\pi^4}|V_{ts}^{\star}V_{tb}|^2\alpha_{em}m_b^5 \times\left\{|\bar{D}|^2+A+\frac{\delta_\gamma^{\rm NP}}{m_b^2}|C_7^{0,\rm eff}(\mu_b)|^2 +\frac{\delta_c^{\rm NP}}{m_c^2}\,{\rm Re}\left[[C_7^{0,\rm eff}(\mu_b)]^* \times\left(C_2^{0,\rm eff}(\mu_b)-\frac{1}{6}\,C_1^{0,\rm eff}(\mu_b)\right)\right]\right\}. \tag{35}$$

Since we work in the new operator basis, a contribution to the term in $1/m_c^2$ comes not only from $\mathcal{O}_2$, as was incorrectly assumed in Ref. [17], but also from $\mathcal{O}_1$. The nonperturbative quantities $\delta_\gamma^{\rm NP}$ [23] and $\delta_c^{\rm NP}$ [26] in Eq. (35) are

$$\delta_\gamma^{\rm NP}=\frac{\lambda_1}{2}-\frac{9\lambda_2}{2},\quad \delta_c^{\rm NP}=-\frac{\lambda_2}{9}, \tag{36}$$

where λ_1 and λ_2 parametrize the kinetic energy of the b quark and the chromomagnetic interactions, respectively. Their values are $\lambda_1=-0.5\ {\rm GeV}^2$ and $\lambda_2=-0.12\ {\rm GeV}^2$. Of these two parameters, the first has larger uncertainties than the second one. As will appear from the final formula for $B(\bar{B}\to X_s\gamma)$, the overall λ_1 dependence cancels to a large extent.

The branching ratio is then obtained as

$$B(\bar{B}\to X_s\gamma)=\frac{\Gamma(\bar{B}\to X_s\gamma)}{\Gamma_{\rm SL}}\,B_{\rm SL}, \tag{37}$$

where $B_{\rm SL}$ is the measured semileptonic branching ratio and the semileptonic decay width $\Gamma_{\rm SL}$ is given by

$$\Gamma_{\rm SL}=\frac{G_F^2}{192\pi^3}|V_{cb}|^2m_b^5g(z)\left(1-\frac{2\alpha_S(\bar{\mu}_b)}{3\pi}\,f(z)+\frac{\delta_{\rm SL}^{\rm NP}}{m_b^2}\right);\qquad z=\frac{m_c^2}{m_b^2}. \tag{38}$$

The phase space function $g(z)$ and the (approximated) QCD-radiation function $f(z)$ [45] in Eq. (38) are

$$g(z)=1-8z+8z^3-z^4-12z^2\ln z,\qquad f(z)=\left(\pi^2-\frac{31}{4}\right)(1-\sqrt{z})^2+\frac{3}{2} \tag{39}$$

and the nonperturbative correction $\delta_{\rm SL}^{\rm NP}$ reads [24,25]

$$\delta_{\rm SL}^{\rm NP}=\frac{\lambda_1}{2}+\frac{3\lambda_2}{2}\left[1-4\,\frac{(1-z)^4}{g(z)}\right]. \tag{40}$$

In Eq. (38) $\bar{\mu}_b$ is the renormalization scale relevant to the semileptonic process, which is *a priori* different from the renormalization scale μ_b in the radiative decay, as stressed in Ref. [27]. However, as pointed out in Ref. [46], the identification $\bar{\mu}_b=\mu_b$ turns out to be more conservative. We therefore use $\bar{\mu}_b=\mu_b$ in the numerical analysis. Furthermore, in the evaluation of Eq. (37), we do not expand $1/\Gamma_{\rm SL}$ in powers of α_S.

IV. RESULTS

In this section we discuss results and theoretical uncertainties of the NLO calculation of $B(\bar{B}\to X_s\gamma)$ in 2HDMs. As will be shown, these uncertainties can be very large, in contrast with what is found in the SM. For reference, we give our SM result

$$B(\bar{B}\to X_s\gamma)=[3.57\pm^{0.01}_{0.12}(\mu_b)\pm^{0.00}_{0.08}(\mu_W)\pm^{0.29}_{0.27}({\rm param})]\times10^{-4}. \tag{41}$$

The central value 3.57×10^{-4} is obtained for $\mu_b=4.8$ GeV, $\mu_W=M_W$ and the central values of the input parameters listed in Table I of Appendix F. The low-scale variation in the interval [2.4,9.6] GeV gives the maximum value for $B(\bar{B}\to X_s\gamma)$ at $\mu_b=4.2$ GeV and the minimum at $\mu_b=9.6$ GeV. The matching scale dependence of the branching ratio is monotonically decreasing for increasing μ_W: from the central value in Eq. (41) $B(\bar{B}\to X_s\gamma)$ is reduced by 2% at $\mu_W=m_t$. The value 3.57×10^{-4} in Eq. (41) reduces to 3.46×10^{-4} when the factor $1/\Gamma_{\rm SL}$ in Eq. (37) is expanded in α_S.

Our results for the branching ratio $B(\bar{B}\to X_s\gamma)$ in the class of 2HDMs considered, is parametrized in terms of $\{X,Y,m_H\}$. We limit the range of this three-dimensional parameter space as follows. We fix Y to small real values of $\mathcal{O}(1)$ and scan X in the complex plane without ever violating the perturbativity requirement on X and Y discussed in Ref. [32]. As explained in Ref. [47], the value of m_H in 2HDMs can be as low as the LEP I lower bound of 45 GeV. We do not strictly apply cuts on $\{X,Y,m_H\}$ due to the measurement of R_b or of other processes such as B-$\bar{B}$ mixing with virtual exchange of charged Higgs bosons, which could remove some corners of the parameter space considered. Our interest is more to show some theoretical features of the NLO calculation of $B(\bar{B}\to X_s\gamma)$ in regions as wide as possible and to discuss constraints due to the decay $\bar{B}\to X_s\gamma$ itself. For the numerical evaluations, unless otherwise specified, we use the central value of the input parameters listed in Table I in Appendix F. The values of the matching and low scale, chosen respectively in the intervals $[M_W,\max(m_t,m_H)]$ and [2.4, 9.6] GeV, are explicitly given for each result presented.

In order to investigate the reliability of the NLO prediction for the branching ratio, we study the term $|\bar{D}|^2$, which dominates the expression within curly brackets in Eq. (35). Notice that $|\bar{D}|^2$ encapsulates all the matching scale dependence and the bulk of the dependence on the low scale. At the NLO level, the procedure of squaring $\bar{D}$ dictated by perturbation theory, in which terms of $\mathcal{O}(\alpha_S^2)$ are omitted, gives

$$|\bar{D}|^2=|C_7^{0,\rm eff}(\mu_b)|^2\{1+2\,{\rm Re}(\Delta\bar{D})\}, \tag{42}$$

where $\Delta\bar{D}$ is defined as [see Eq. (29)]

$$\Delta\bar{D} \equiv \frac{\bar{D} - C_7^{0,\mathrm{eff}}(\mu_b)}{C_7^{0,\mathrm{eff}}(\mu_b)} = \left(\frac{\alpha_S(\mu_b)}{4\pi}\right) \frac{C_7^{1,\mathrm{eff}}(\mu_b) + V(\mu_b)}{C_7^{0,\mathrm{eff}}(\mu_b)}. \tag{43}$$

If $|\Delta\bar{D}|$ is not small, the formally next to next to leading order (NNLO) term $|\Delta\bar{D}|^2$, dropped in Eq. (42), is numerically relevant. Its omission can lead to branching ratios with a large dependence on μ_b, or in extreme cases, even to negative values for the branching ratio. In these situations, the truncation of the perturbative expansion of $\bar{D}$ at the NLO level is certainly not justified. As we shall see, the size of $|\Delta\bar{D}|$ depends crucially on the values of X, Y, and m_H. We split our analysis as follows. In Sec. IV A, we disentangle the effect of the couplings X and Y by studying the NLO contributions to the Higgs components $\bar{D}_{XY}$ and $\bar{D}_{YY}$ of the reduced amplitude $\bar{D}$. In Sec. IV B we illustrate predictions for the branching ratio for real X and Y couplings, giving particular emphasis to cases in which the results are highly unstable or altogether unacceptable. In Sec. IV C we discuss in detail type-II models, for which the NLO corrections are under control, and type-I models for which the reliability of the theoretical prediction depends strongly on the point of parameter space considered. Finally, in Sec. IV D, we study branching ratios and *CP* asymmetries in the presence of complex couplings, and outline regions of parameter space where these predictions are trustworthy.

A. Amplitude: X-Y independent analysis

Before analyzing the size of the various corrections within 2HDMs, it is worth reviewing the situation in the SM. There, as it is was first observed in Ref. [21], the NLO contribution to the matching condition tends to cancel the contribution due to the NLO evolution from the matching scale μ_W to the low-energy scale μ_b (see upper frame in Fig. 1). Indeed, $C_{7,\mathrm{SM}}^{1,\mathrm{eff}}$, which is 12% of $C_{7,\mathrm{SM}}^{0,\mathrm{eff}}$ at μ_W, is practically negligible for $\mu_b \in [2.4, 9.6]$ GeV. The dominant NLO effect is therefore due to $V_{\mathrm{SM}}(\mu_b)$ which, in the same range of μ_b, is at most 20% of the leading term $C_{7,\mathrm{SM}}^{0,\mathrm{eff}}(\mu_b)$ and vanishes exactly at $\mu_b \sim 3.5$ GeV. These features are illustrated in Fig. 2. The size of $V_{\mathrm{SM}}(\mu_b)$ results from cancellations among the individual contributions of the four operators $\mathcal{O}_1$, $\mathcal{O}_2$, $\mathcal{O}_7$, and $\mathcal{O}_8$ retained in Eq. (30). The details of the above described cancellations and, more generally, of the distribution of the complete NLO correction among the individual terms in Eq. (29), are specific to the $\overline{\mathrm{MS}}$ scheme (with anticommuting γ_5) and could be altered by a different choice of scheme. We remind that only the complete $\bar{D}_{\mathrm{SM}}$ term as well as the final $B(\bar{B} \to X_s\gamma)$ are scheme independent, up to higher order.

One is naturally led to ask whether the cancellations among different sets of NLO corrections observed in the SM are spoiled in 2HDMs. To address this issue, we investigate the building blocks $\bar{D}_{XY}$ and $\bar{D}_{YY}$ defined in Eq. (31), for a specific value of m_H. In Fig. 2, we show the real parts of

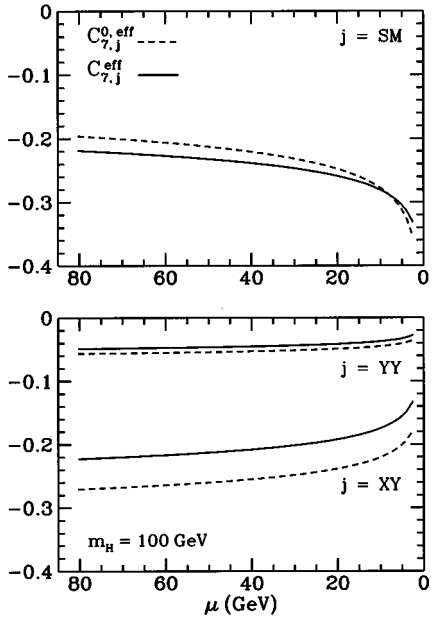

FIG. 1. RGE evolution of the Wilson coefficients C_7^{eff}, at the LO (with NLO α_S) (dashed lines) and at the NLO (solid lines), for $\mu_W = M_W$. The upper frame shows the SM coefficients, the lower one the coefficients $C_{7,YY}^{\mathrm{eff}}$, $C_{7,XY}^{\mathrm{eff}}$, for $m_H = 100$ GeV. The needed input parameters are fixed at their central values listed in Table I in Appendix E.

$\bar{D}_{XY}$ and $\bar{D}_{YY}$ for $m_H = 100$ GeV, together with the real part of $\bar{D}_{\mathrm{SM}}$. Even when considering real X and Y couplings, imaginary parts to $\bar{D}$ come from the absorptive terms of the loop corrections in Eq. (30). As it can be seen from Eq. (42), the imaginary parts of $\bar{D}_{XY}$, $\bar{D}_{YY}$, and $\bar{D}_{\mathrm{SM}}$ do not contribute to $B(\bar{B} \to X_s\gamma)$ at this order of perturbation theory if X and Y are real. In the remainder of this section, therefore, any reference to these components is understood as a reference to their real parts.

Unlike in the SM, the NLO corrections coming from $C_{7,XY}^{1,\mathrm{eff}}(\mu_b)$ and $V_{XY}(\mu_b)$, have roughly the same size ($\sim$20%) and the same sign, for $m_H = 100$ GeV. The combined correction

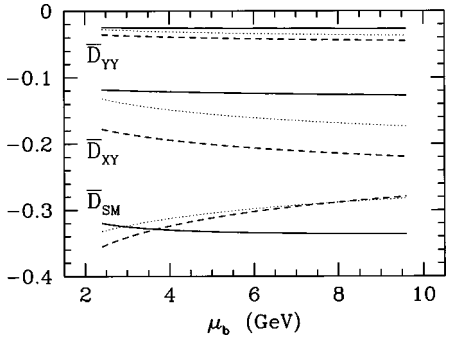

FIG. 2. Low-scale dependence of the term $\bar{D}$ (solid line) of the LO coefficient $C_7^{0,\mathrm{eff}}(\mu_b)$ (with NLO α_S) (dashed line), and of $C_7^{\mathrm{eff}}(\mu_b)$ (dotted lines), for $\mu_W = M_W$. For $\bar{D}_{XY}$ and $\bar{D}_{YY}$, the value $m_H = 100$ GeV was used. The needed input parameters are fixed at their central values listed in Table I in Appendix F.

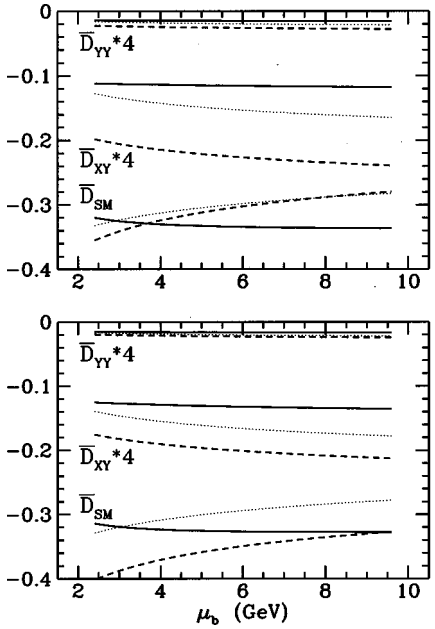

FIG. 3. Low-scale dependence of the term $\bar{D}$ (solid lines) of the LO coefficient $C_7^{0,\mathrm{eff}}(\mu_b)$ (with NLO α_S) (dashed lines), and of $C_7^{\mathrm{eff}}(\mu_b)$ (dotted lines), for $m_H=500$ GeV. The matching scale $\mu_W=M_W$ is used in the upper frame and $\mu_W=m_H$ in the lower one. The needed input parameters are fixed at their central values listed in Table I in Appendix F.

$$\Delta\bar{D}_{XY}\equiv\frac{\bar{D}_{XY}-C_{7,XY}^{0,\mathrm{eff}}(\mu_b)}{C_{7,XY}^{0,\mathrm{eff}}(\mu_b)}=\left(\frac{\alpha_S(\mu_b)}{4\pi}\right)\frac{C_{7,XY}^{1,\mathrm{eff}}(\mu_b)+V_{XY}(\mu_b)}{C_{7,XY}^{0,\mathrm{eff}}(\mu_b)}\qquad(44)$$

amounts to the considerable values of -43 to -36 % when varying $\mu_b\in[2.4,9.6]$ GeV. [We warn the reader here that all components of the LO Wilson coefficient $C_7^{0,\mathrm{eff}}(\mu_b)$ discussed in this section and plotted in Figs. 1 and 2, are evaluated with NLO α_S.] Differently than in the SM, there is no scale μ_b in the range considered, at which the LO and NLO prediction for D_{XY} coincide. Similar results hold for D_{YY}.

The change in matching scale from $\mu_W=M_W$ (value used for Fig. 2) to, say, $\mu_W=m_H$, is practically inconsequential for $m_H=100$ GeV. It becomes very relevant for large values of m_H, since it crucially affects the size of the NLO corrections. For $m_H=500$ GeV, as shown in Fig. 3, the correction ΔD_{XY} reduces to -37 and -31 % when varying μ_b in the usual interval [2.4,9.6] GeV, whereas values of -51 and -45 % are obtained for $\mu_W=M_W$. Notice that, for $m_H=500$ GeV, $|D_{XY}|$ is roughly ten times smaller than $|D_{\mathrm{SM}}|$ and D_{YY} completely negligible. When using the same matching scale $\mu_W=500$ GeV for the SM contribution, the cancellation between the NLO correction to the matching condition and the NLO evolution of the Wilson coefficient $C_{7,\mathrm{SM}}^{\mathrm{eff}}$ does not occur anymore. Large cancellations are instead observed between $V_{\mathrm{SM}}(\mu_b)$ and $C_{7,\mathrm{SM}}^{1,\mathrm{eff}}(\mu_b)$. The complete correction $|\Delta\bar{D}_{\mathrm{SM}}|$ ranges still between 19 and 2 % for $\mu_b\in[2.4,9.6]$ GeV, but the point where NLO and LO predictions for D_{SM} coincide is pushed to the higher end of μ_b. These results imply that for heavy H^+ and large enough X and Y couplings [to lift at least D_{XY} to be of $\mathcal{O}(D_{\mathrm{SM}})$], a choice of μ_W of $\mathcal{O}(m_H)$, instead than $\mathcal{O}(M_W)$, minimizes the size of the NLO corrections.

We draw attention to the fact that the sensitivity of the reduced amplitude $\bar{D}$ to m_H is weaker than that of the Wilson coefficient $C_7^{\mathrm{eff}}(\mu_W)$ at the matching scale. It is interesting to see that the coefficients $C_{7,\mathrm{SM}}^{\mathrm{eff}}$ and $C_{7,XY}^{\mathrm{eff}}$ are almost identical at the matching scale μ_W for $m_H=100$ GeV. This feature is clearly visible in Fig. 1, where the matching scale $\mu_W=M_W$ is used. (It remains true for all $\mu_W\in[M_W,m_t]$.) We observe in Fig. 1 that the RGE flow from μ_W to μ_b introduces a large gap between $C_{7,\mathrm{SM}}^{\mathrm{eff}}(\mu_b)$ and $C_{7,XY}^{\mathrm{eff}}(\mu_b)$, which is then somewhat widened at the level of the reduced amplitude $\bar{D}$ by the inclusion of the $V(\mu_b)$ contribution. At $\mu_b\in[2.4,9.6]$ GeV, $\bar{D}_{XY}$ is about a factor of three smaller than $\bar{D}_{\mathrm{SM}}$.

When going to physical observables such as $B(\bar{B}\to X_s\gamma)$, the individual building blocks of $\bar{D}$, discussed above in a coupling-independent way, are weighted according to the values of the couplings X and Y.

B. Branching ratio: Real couplings

The almost perfect flatness of $\bar{D}_{YY}$ and $\bar{D}_{XY}$ shown in Figs. 2 and 3, should not lead to the conclusion that the NLO prediction for $B(B\to X_s\gamma)$ is well behaved. It was explicitly shown in Ref. [27], by expanding the Wilson coefficients around $\mu_b=m_b$, that the dominant scale dependence of the form $\alpha_S(m_b)\ln(\mu_b/m_b)$ is cancelled in the complete NLO expression for $\bar{D}$ in Eq. (29) and consequently also in $|\bar{D}|^2$. If the NLO corrections are large enough to reduce substantially the magnitude of the LO term, $|\bar{D}|^2$ becomes sensitive to higher order dependence on μ_b of the form $\alpha_S^2(m_b)\ln^p(\mu_b/m_b)$ $(p=1,2)$. The flatness of $\bar{D}$ seems to indicate that the omitted NNLO term $|\Delta\bar{D}|^2$ would cancel to a large extent this remaining μ_b dependence. Nevertheless, whether the omitted $|\Delta\bar{D}|^2$ in Eq. (42) is the bulk of the NNLO corrections can only be decided when a complete NNLO calculation is at hand.

It is clear that the reliability of the NLO prediction for the branching ratio, which is linked to the size of $\Delta\bar{D}$, depends on the values of X and Y. For a given m_H, it is possible to choose these couplings in such a way that the reduced amplitude $\bar{D}$ is dominated, for example, by the Higgs contribution D_{XY}. For such points in the parameter space $\{X,Y,m_H\}$, the size of the NLO corrections to the branching ratio is then roughly 2 $\mathrm{Re}(\Delta D_{XY})$, i.e., about -80% for $m_H=100$ GeV. In this case, the NLO corrections substantially reduce the leading order prediction. As expected, the resulting scale dependence of the branching ratio $B(B\to X_s\gamma)$ is large, viz. about 40%. For $Y=1$ and the same value of m_H, D_{XY} completely dominates the branching ratio for $|X|\geqslant 20$, outside the range shown in Figs. 4. The prediction for $B(B\to X_s\gamma)$ is then,

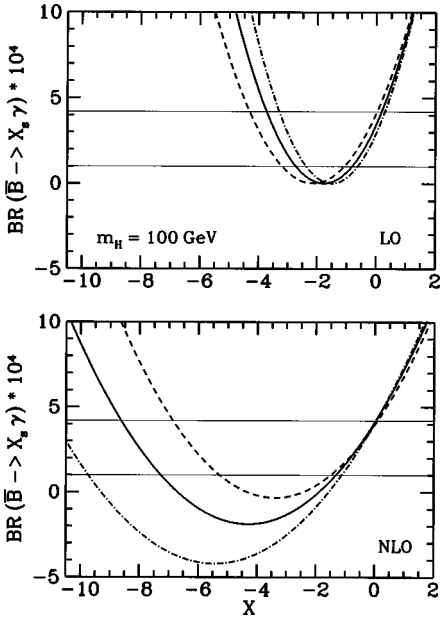

FIG. 4. Branching ratio as a function of the coupling X, for $Y=1$ and $m_H=100$ GeV. The upper (lower) frame shows the LO (NLO) result for $\mu_b=4.8$ GeV (solid lines), $\mu_b=2.4$ GeV (dashed lines), and $\mu_b=9.6$ GeV (dash-dotted lines), and matching scale $\mu_W=m_H=100$ GeV. The needed input parameters are fixed at their central values listed in Table I in Appendix F. Superimposed is the range of values allowed by the CLEO measurement.

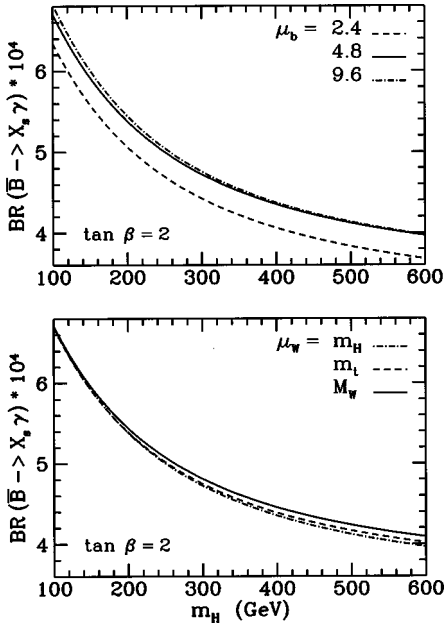

FIG. 5. Branching ratio as a function of m_H in a 2HDM of type II, for three different choices of the low scale: $\mu_b=2.4$, 4.8, 9.6 GeV and $\mu_W=m_H$ (upper frame), and for for three different choices of the matching scale $\mu_W=M_W$, m_t, m_H, and $\mu_b=4.8$ GeV. The needed input parameters are fixed at their central values listed in Table I in Appendix F.

however, far above the band of values allowed by the CLEO measurement.

Moreover, it is possible to choose X and Y in such a way that $\mathrm{Re}(\Delta D)<-50\%$. As Eq. (42) shows, this choice leads to a negative NLO prediction for $B(B\to X_s\gamma)$. Needless to say, in such a situation higher order corrections to the NLO calculation are mandatory to obtain sensible results. In our representative case of $m_H=100$ GeV and $Y=1$ illustrated in Fig. 4, the range of X corresponding to a negative branching ratio is roughly $-10<X<-2$. A comparison with the upper frame of this figure shows that, given the very large scale dependence of the LO calculation, one could have guessed the pathological situation which is encountered at the NLO level.

Reliable predictions for the branching ratio with a mild scale dependence are obtained only for $X>-1$ (see lower frame of Fig. 4). For these values, the SM contribution dominates, but the Higgs contribution proportional to XY^* is still large enough to produce a sharp raise of $B(B\to X_s\gamma)$ when X increases from -1 to 2. Notice that for $Y=1$ the values $X=-1$ and $X=1$ correspond respectively to the ordinary 2HDM of type I and type II with $\tan\beta=1$. Type-I models, however, are not always so stable and well behaved as in the case described above. For $Y=1$ and $X=-1$ (corresponding to $\tan\beta=1$), it is enough to lower m_H to 45 GeV to find a low-scale dependence of $^{+40\%}_{-60\%}$ (see Fig. 7). Keeping m_H at 100 GeV and increasing Y to 2, we find that for $X=-2$ (corresponding to a type-I model with $\tan\beta=0.5$), the branching ratio is negative for all values of $\mu_b \in [2.4,9.6]$ GeV.

Going to heavier Higgs masses, e.g., $m_H=500$ GeV, we find for $Y=1$ the same qualitative features as in Fig. 4, but shifted to larger ranges of $|X|$. We should warn the reader, however, that for large enough $|X|$, when the Higgs contribution dominates over the SM one, the stability of the branching ratio becomes worse. The NLO corrections have a more dramatic dependence on the particular matching scale chosen, than in the case $m_H=100$ GeV. Indeed, for $\mu_W=m_H=500$ GeV, the relevant correction for the branching ratio $2\,\mathrm{Re}(\Delta D_{XY})$ is $\sim-70\%$, but exceeds -100% for $\mu_W=M_W$.

C. Type-I and type-II models

Theoretical predictions for the branching ratio in type-II models stand, in general, on rather solid ground. In Fig. 5, we show these predictions in a type-II model with $\tan\beta=2$, for $100\leqslant m_H\leqslant 600$ GeV. This value of $\tan\beta$ is particularly interesting since already for $\tan\beta\geqslant 2$, the branching ratio becomes insensitive to the actual value of this variable: the contribution D_{YY} is, in fact, suppressed by the coupling $|Y|^2\leqslant 1/4$, whereas the contribution D_{XY} is multiplied by the coupling $XY^*=1$, for any value of $\tan\beta$. For $\tan\beta\leqslant 2$, the branching ratio grows very rapidly when $\tan\beta$ decreases and can be made compatible with existing measurements only for large values of m_H.

The upper frame of Fig. 5 shows the low-scale dependence of $B(B\to X_s\gamma)$ for matching scale $\mu_W=m_H$, for $m_H>100$ GeV. It is less than 10% for any value of m_H above the lower bound at the CERN e^+e^- collider LEP of 45 GeV. Such a small scale uncertainty is a generic feature of type-II

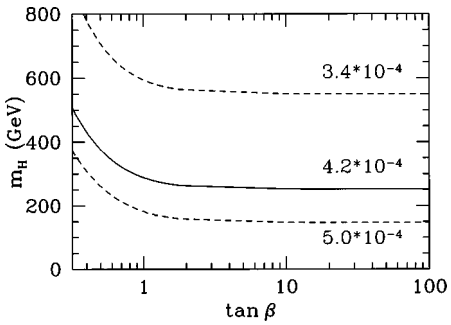

FIG. 6. Contour plot in (tan β,m_H) obtained by using the NLO expression for the branching ratio $B(B\to X_s\gamma)$ and possible experimental upper bounds (see text). The allowed region is above the corresponding curves.

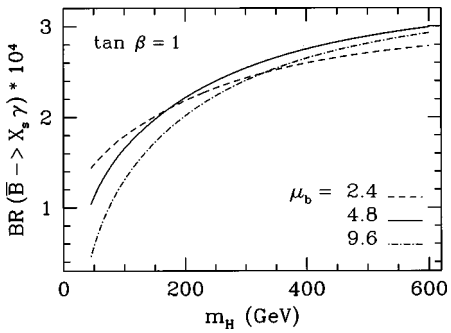

FIG. 7. Branching ratio as a function of m_H in a 2HDM of type I, for three different choices of the low scale: $\mu_b=2.4$, 4.8, 9.6 GeV and for $\mu_W=m_H$. The needed input parameters are fixed at their central values listed in Table I in Appendix F.

models and remains true for values of tan β as small as 0.5. The lower frame in Fig. 5 shows the (very weak) matching scale dependence as obtained by varying μ_W in the interval $[M_W,\max(m_t,m_H)]$. We point out that the lowest estimate of $B(B\to X_s\gamma)$ comes from the largest value of μ_W in this interval.

In type-II models, the theoretical estimate of $B(\bar{B}\to X_s\gamma)$ can be well above the range $(1-4.2)\times10^{-4}$ indicated by the CLEO Collaboration as the band of experimentally allowed values. It is therefore interesting to establish with some accuracy which values of $\{\tan\beta,m_H\}$ are excluded by possible measurements of the branching ratio $B(\bar{B}\to X_s\gamma)$. Our results are given in Fig. 6, where we show the contour of the region excluded by the upper bound obtained by CLEO, 4.2×10^{-4}, as well as for other two hypothetical values, 3.4×10^{-4} and 5.0×10^{-4}; the latter one is not far from the upper bound obtained by the ALEPH Collaboration. These contours are obtained by finding the minimum of $B(\bar{B}\to X_s\gamma)$, when varying simultaneously the input parameters within their errors (see Table I in Appendix F) and the two scales μ_b and μ_W in the ranges $2.4\leqslant\mu_b\leqslant9.6$ GeV and $M_W\leqslant\mu_W\leqslant\max(m_t,m_H)$. For tan β=0.5, 1, 5, we exclude respectively $m_H\leqslant375$, 289, 255 GeV. Notice that the flatness of the curves shown in Fig. 5 towards the higher end of m_H, causes a high sensitivity of these bounds on all details of the calculation. Different treatments of the infrared singularities when the photon gets soft (e.g., with a cut in the photon energy [21]) and the possible expansion of $1/\Gamma_{SL}$ in powers of α_S could alter the branching ratio at the 1% level, i.e., well within the estimated theoretical uncertainty. These details, however, could still produce shifts of several tens of GeV, in either direction, in the lower bounds quoted above.

Branching ratios in type-I models can be reliably predicted for $m_H>100$ GeV and tan $\beta>1$. Theoretical results for this range of parameters fall within the CLEO band $(1-4.2)\times10^{-4}$, as it can be seen in Fig. 7 for tan β=1 and $100\leqslant m_H\leqslant600$ GeV. Larger values of tan β decrease the Higgs contribution to the branching ratio, giving therefore values closer to the SM prediction. Lower values of m_H (and/or tan $\beta<1$) can produce results outside the CLEO range. For these parameters, however, the theoretical predictions are unstable under scale variation and, at times, ill defined. As shown in Fig. 7, a scale dependence of $^{+40\%}_{-60\%}$ is obtained for $m_H=45$ GeV and tan β=1. For tan $\beta<1$, negative values of the branching ratio are found already for $m_H=100$ GeV.

D. Branching ratio: Complex couplings and rate asymmetries

In this section we study several aspects of the decay $\bar{B}\to X_s\gamma$ in the presence of complex X and Y couplings. Particularly motivating is the observation that the measurement of $B(\bar{B}\to X_s\gamma)$ yields strong constraints on Im(XY*) [31,32]. In turn, these constraints limit the possibility of having large indirect CP asymmetries in neutral B decays such as $B\to\psi K_S$ [32]. This observation is based on a LO analysis whose reliability and stability under scale variation was not enquired. We plan to investigate this aspect and to check how the bound in Ref. [32] may be modified by the inclusion of NLO corrections.

The bound of Ref. [32] on Im(XY*) is obtained as follows. Since the LO branching ratio is proportional to $|C_7^{0,\mathrm{eff}}(\mu_b)|^2$, the upper bound $B(B\to X_s\gamma)\leqslant4.2\times10^{-4}$ from the CLEO measurement implies an upper bound on $|C_7^{0,\mathrm{eff}}(\mu_b)|^2$, and therefore on Im($XY$*) when

$$\begin{aligned}C_7^{0,\mathrm{eff}}(\mu_b)&=\{C_{7,\mathrm{SM}}^{0,\mathrm{eff}}(\mu_b)+|Y|^2C_{7,YY}^{0,\mathrm{eff}}(\mu_b)\\&\quad+\mathrm{Re}(XY^*)C_{7,XY}^{0,\mathrm{eff}}(\mu_b)\}+i\ \mathrm{Im}(XY^*)C_{7,XY}^{0,\mathrm{eff}}(\mu_b)\\&=i\ \mathrm{Im}(XY^*)C_{7,XY}^{0,\mathrm{eff}}(\mu_b),\end{aligned}\tag{45}$$

i.e., when the real parts of the charged Higgs contributions cancel the SM coefficient $C_{7,\mathrm{SM}}^{0,\mathrm{eff}}(\mu_b)$. An inspection of the upper frame of Fig. 4 shows that, for $m_H=100$ GeV and $Y=1$, a vanishing branching ratio is induced by the real coupling $X=-2$. The choice of complex couplings X and Y with $Y=1$ and Re $X=-2$, therefore, fulfills to a good approximation the condition (45), for all values of Im X. The corresponding branching ratio, obtained with the central value of the input parameters, $\mu_W=m_H$, and $\mu_b=m_b$, and shown in Fig. 8 as a function of Im X, equals 4.2×10^{-4} at $|\mathrm{Im}\,X|\sim2$. For the chosen Higgs boson mass, $m_H=100$ GeV, therefore, the upper bound on $|\mathrm{Im}(XY^*)|$ is ~2. Notice that this

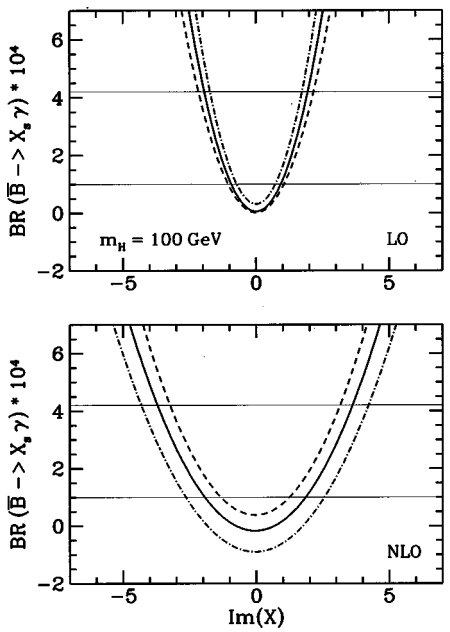

FIG. 8. Branching ratio as a function of Im X, with fixed Re $X=-2$ and $Y=1$, for $\mu_W=m_H$ and different low scales: $\mu_b=4.8$ GeV (solid lines), $\mu_b=2.4$ GeV (dashed lines), and $\mu_b=9.6$ GeV (dash-dotted lines). The needed input parameters are fixed at their central values listed in Table I in Appendix F. Superimposed is the range of values allowed by the CLEO measurement. The upper (lower) frame shows the LO (NLO) result.

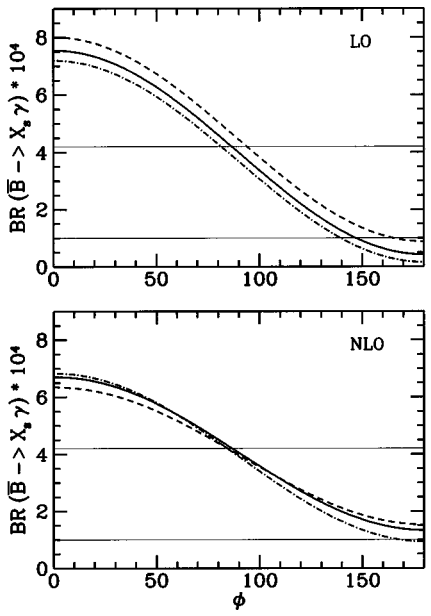

FIG. 9. Branching ratio as a function of ϕ, where ϕ parametrizes X: $X=2\exp(i\phi)$, for $Y=\frac{1}{2}$, $m_H=100$ GeV, and $\mu_W=m_H$. Solid, dashed, and dash-dotted lines correspond, respectively, to $\mu_b=4.8$, 2.4, and 9.6 GeV. The needed input parameters are fixed at their central values listed in Table I in Appendix F. Superimposed is the range of values allowed by the CLEO measurement. The upper (lower) frame shows the LO (NLO) result.

procedure yields only a first estimate for the actual LO bound, since the errors of the input parameters have not been considered.

We observe that a variation of the low-scale μ_b in the usual range leads to large uncertainties for the branching ratio, throughout the whole range of Im X. In particular, for $|\mathrm{Im}\,X|\sim 2$, this uncertainty amounts to $\pm 25\%$. When including NLO corrections, the situation does not improve, as the lower frame of Fig. 8 shows. It is interesting to see that the value of $B(B\to X_s\gamma)$ for $\mu_b=m_b$, at $|\mathrm{Im}\,X|\sim 2$ drops from 4.2×10^{-4} to roughly 1×10^{-4}. The intersection of the NLO curve for $\mu_b=m_b$ with the CLEO upper bound is at Im $X\sim 4$. This procedure is essentially the construction of the NLO bound for $|\mathrm{Im}(XY^*)|$ in the sense specified before. (In the actual construction, one should have cancelled also small real parts of $C_7^{0,\mathrm{eff}}$ with NLO α_s and small terms coming from absorptive parts of virtual corrections.)

The inclusion of NLO corrections verifies explicitly the instability of the LO upper bound on $\mathrm{Im}(XY^*)$. Given the fact that the NLO predictions for $B(B\to X_s\gamma)$ are plagued by even larger scale uncertainties, it is hard to believe that the NLO candidate qualifies as a reliable bound.

Not all complex X and Y couplings yield NLO predictions as problematic as those shown in Fig. 8. A typical case in which the perturbative expansion of $B(B\to X_s\gamma)$ can be safely truncated at the NLO level is identified by: $Y=1/2$, $X=2\exp(i\phi)$, and $m_H=100$ GeV. Indeed, for these parameters, the real and imaginary part of $|Y|^2 D_{YY}$ and $(XY^*)D_{XY}$ are dominated by D_{SM}. Therefore, the low-scale dependence of the branching ratio is not much larger than the very mild one obtained for the SM estimate, as shown in Fig. 9. This case is particularly interesting since it gives rise to a theoretical prediction of $B(\bar{B}\to X_s\gamma)$ consistent with the CLEO measurement, even for a relatively small value of m_H. Such a light charged Higgs boson can contribute to the decays of the t quark, through the mode $t\to H^+ b$.

We now investigate *CP* asymmetries induced by complex couplings. It is well known that in the SM a nonvanishing direct *CP* rate asymmetry

$$a_{CP}=\frac{B(\bar{B}\to X_s\gamma)-B(B\to\bar{X}_s\gamma)}{B(\bar{B}\to X_s\gamma)+B(B\to\bar{X}_s\gamma)} \tag{46}$$

is due to nontrivial relative weak and relative strong phases in the decay amplitude for $b\to s\gamma$ (as well as the one for $b\to s\gamma g$). We write the amplitude of $b\to s\gamma$ and of the *CP* conjugated process as

$$\mathcal{A}(b\to s\gamma)=(V_{ub}V_{us}^*)A_u+(V_{cb}V_{cs}^*)A_c+(V_{tb}V_{ts}^*)A_t,$$

$$\mathcal{A}(\bar{b}\to\bar{s}\gamma)=(V_{ub}V_{us}^*)^*A_u+(V_{cb}V_{cs}^*)^*A_c+(V_{tb}V_{ts}^*)^*A_t, \tag{47}$$

where the dependence on the CKM matrix is manifest. Working in the LO approximation, the quantities A_u, A_c, and A_t are real, hence $|\mathcal{A}(\bar{b}\to\bar{s}\gamma)|^2=|\mathcal{A}(b\to s\gamma)|^2$, and consequently $a_{CP}=0$. Relative strong phases among A_u, A_c, and A_t only appear at the NLO level, due to absorptive terms in the loop diagrams. Thus, a nonvanishing *CP* asym-

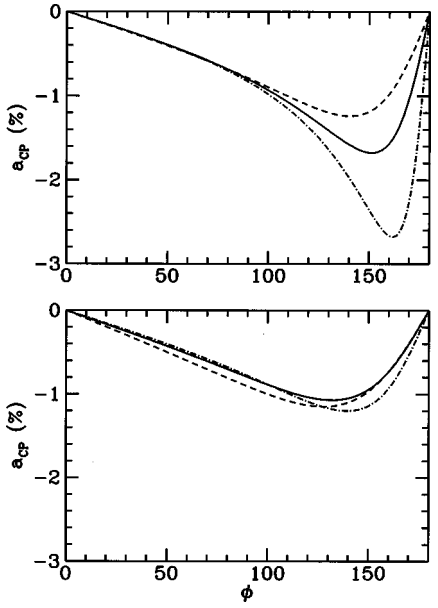

FIG. 10. *CP* rate asymmetry a_{CP} as a function of ϕ, where ϕ parametrizes X: $X=2\exp(i\phi)$, for $Y=\frac{1}{2}$, $m_H=100$ GeV, and $\mu_W=m_H$. Solid, dashed, and dash-dotted lines correspond, respectively, to $\mu_b=4.8$, 2.4, and 9.6 GeV. The needed input parameters are fixed at their central values listed in Table I in Appendix F. In the upper (lower) frame the LO (NLO) expression for the denominator in Eq. (46) is used. See text for more details.

metry results if $V_{ub}V_{us}^*$, $V_{cb}V_{cs}^*$, and $V_{tb}V_{ts}^*$ have also relative phases. In the approximation $V_{ub}V_{us}^*=0$, which we used so far, the *CP* asymmetry vanishes, since unitarity implies that $V_{cb}V_{cs}^*=-V_{tb}V_{ts}^*$. Undoing this approximation, the SM *CP* rate asymmetry turns out to be below 1% [48].

Since the *CP* rate asymmetry is so tiny in the SM, it would be exciting if the imaginary parts of the X and Y couplings would induce—together with the absorptive parts of the NLO loop functions—measurable *CP* rate asymmetries. In order to investigate this question, we switch off the SM asymmetry by working in the limit $V_{ub}V_{us}^*=0$. As an illustrative example we calculate the *CP* asymmetries for the same values of parameters as in Fig. 9, i.e., for $X=2\exp(i\phi)$, $Y=\frac{1}{2}$, and for $m_H=100$ GeV, where the branching ratio appears to be well behaved. As mentioned above, the NLO prediction for the branching ratio in the numerator of Eq. (46) is required to obtain the first nonvanishing term for the rate asymmetry. For the denominator, one can either use the LO or the NLO estimate for the two branching ratios. The difference amounts to higher order terms which are not systematically calculated. The respective results are shown in the upper and lower frame in Fig. 10 as a function of ϕ. For this specific choice of X and Y the asymmetries are rather modest, at the 1% level. The scale dependence shown by the lower frame is certainly smaller than that in the upper frame. However, since both procedure are in principle viable, one cannot conclude that the result for the *CP* asymmetries is as reliable as indicated in the lower frame. Although we have not systematically scanned the parameter space $\{X,Y,m_H\}$, this is our generic result: choices of couplings X and Y which render the branching ratio stable, i.e., not plagued by a large dependence on the scale μ_b, induce small values of a_{CP}.

V. CONCLUSIONS

We have presented NLO predictions for the decay $\bar{B}\to X_s\gamma$ in generic 2HDMs with flavor-conserving tree-level neutral couplings. We include in this definition multi-Higgs-doublet models where all charged Higgs bosons, except one, are heavy and completely decoupled at the electroweak scale. Their existence leaves an imprint only in the Yukawa potential where the couplings X and Y multiplying respectively the down and up term are not necessarily correlated, and in general complex. This generalization allows a simultaneous study of $B\to X_s\gamma$ for different types of 2HDMs by continuously varying the couplings X and Y. Results for the well-known type-I and type-II models are then obtained for specific choices of real couplings: only one combination of X and Y, usually denoted as $\tan\beta$, occurs. Since supersymmetric models have an enlarged Higgs sector with two Higgs doublets of type II, the results presented here are also a first step towards a complete evaluation of the rate of $B\to X_s\gamma$ in these models. They constitute already a good approximation for those supersymmetric scenarios, such as gauge-mediated supersymmetric models with large $\tan\beta$, where the Higgs contribution dominates by far over the genuinely supersymmetric contributions [49].

Our calculation is carried out using the effective Hamiltonian formalism with on-shell operators. The NLO matching condition for the decay $B\to X_s\gamma$ was already completely calculated in Ref. [17] and partially in Ref. [33]. For the Wilson coefficients $C_7^{\rm eff}(\mu_w)$ and $C_8^{\rm eff}(\mu_w)$, we find agreement with the existing results. Consensus is also reached in the final version of Refs. [27,17] on the form of $C_1^{\rm eff}(\mu_w)$ and $C_4^{\rm eff}(\mu_w)$ which we present in this paper. We give a generalized solution of the RGE needed to obtain the coefficient $C_7^{\rm eff}(\mu_b)$ at the low-scale μ_b for values of μ_w different from M_w. We correct the dependence on the Wilson coefficients of one of the nonperturbative contribution to $\Gamma(B\to X_s\gamma)$, which is erroneously reported in Ref. [17].

We have given predictions for $B(B\to X_s\gamma)$ in 2HDMs as functions of the parameters $\{X,Y,m_H\}$. We found that the theoretical uncertainties of these NLO calculations are in general larger than those obtained in the SM. The quality of our predictions, therefore, depends strongly on the values of the parameters considered. Before attempting a comparison with the existing experimental data, we summarize the theoretical features of our results. We distinguish several cases. (i) When these parameters are such that the SM contribution is much larger than the Higgs contribution to $B(B\to X_s\gamma)$, the reliability of our predictions does not differ much from that in the SM. This, however, does not prevent $B(B\to X_s\gamma)$ from being rather sensitive to m_H. (ii) For values of parameters which bring the Higgs contributions to the same level as the SM one, with constructive interference between the two, we find in general larger scale dependence than in the SM. (iii) When the Higgs contributions are still of the same order as the SM contribution, but interfere destruc-

tively with it, we find very large scale dependences and, in specific cases, we obtain negative values of $B(\bar{B}\to X_s\gamma)$. (iv) When X and Y make the Higgs contributions largely dominate over the SM one, we find a scale dependence in $B(\bar{B}\to X_s\gamma)$ of $\sim$40% for m_H of $\mathcal{O}(M_W)$. For much larger values of m_H, when $M_W^2 \ll m_H^2$, this scale dependence can improve or worsen according to which value of the matching scale is chosen, i.e., closer to m_H or to M_W. Obviously, models with parameters which induce values of $B(\bar{B}\to X_s\gamma)$ highly instable or negative require the inclusion of higher order QCD corrections before a comparison with experimental results becomes possible.

Type-II models are typical of case (i) and marginally become of case (ii) for m_H at the LEP lower bound of 45 GeV [47] and for tan $\beta\sim 0.5$. The theoretical uncertainty for such models is in general below 10%. Similar uncertainties are obtained for type-I models when m_H and/or tan β are large enough. Rather unstable results are, however, obtained for m_H at the lower end of allowed values and tan $\beta \lesssim \mathcal{O}(1)$. However, in these problematic regions, all predictions obtained for type-I models are consistent with the CLEO measurement of $B(\bar{B}\to X_s\gamma)$. The same is not true for type-II models where the theoretical predictions are always above the SM result. Measurements become then highly constraining. Taking into account only the CLEO result, without combining it with the still preliminary one from ALEPH, we exclude $m_H \leqslant 375$ GeV for tan $\beta=0.5$ and $m_H \leqslant 255$ GeV for tan $\beta=5$. These bounds are very sensitive to details in the definition of the branching ratio (e.g., whether or not it requires an expansion in α_s of $1/\Gamma_{\rm SL}$), which give rise to uncertainties usually not included in the theoretical error for this observable. For the generic 2HDMs which we consider, we find wide regions of parameter space where the theoretical predictions for $B(\bar{B}\to X_s\gamma)$ are reliable and within the band of values $(1.0-4.2)\times 10^{-4}$ allowed by the CLEO measurement. In particular, we find that within these models, charged Higgs bosons can still be light enough to be produced through a decay of the t quark.

Since X and Y are in general complex, new CP violating effects are induced. In particular, the combination Im(XY^*) is important as it may affect the indirect CP asymmetries in $B\to\psi K_s$ already at the LO. It is known that the measurement of $B(\bar{B}\to X_s\gamma)$ constrains Im(XY^*) [31] and an upper bound for this quantity has been obtained in Ref. [32] using the LO calculation. We find that the LO estimate of the branching ratio at the values of X and Y which determine the upper bound extracted in Ref. [32] is unstable under scale variation. The addition of NLO corrections tend to shift the LO bound to a higher value. Nevertheless, the scale dependence of $B(\bar{B}\to X_s\gamma)$ for the new combination of X and Y needed, is still too large to conclude that the bound obtained at the NLO level is stable against higher order corrections. The large instabilities encountered even at this order are due to the fact that the construction of this upper bound requires the almost complete cancellation of the SM contribution.

At the NLO, complex values of X and Y induce also direct CP rate asymmetries, in $\bar{B}\to X_s\gamma$, which is essentially vanishing in the SM. If sizable, a measurement of this observable, could provide a handle to detect some of these models. Unfortunately, we find that combinations of couplings where $B(\bar{B}\to X_s\gamma)$ is reliably predicted, lead to rate asymmetries only at the 1% level.

We find that within 2HDMs, the truncation of the perturbative series at the NLO level is often inappropriate. This is in sharp contrast with the SM case, where the large LO theoretical uncertainties are drastically reduced in the NLO calculation, and the overall size of the NLO corrections is, in comparison, rather modest. It is somehow disturbing to find the problematic features described in this paper in models which structurally do not differ very much from the SM and it is conceivable that other extensions may suffer from the same problems.

ACKNOWLEDGMENTS

We acknowledge discussions with D. Wyler. One of us (F.B.) thanks the Institute of Theoretical Physics of the University of Bern for the hospitality extended to her during several visits while this work was in progress. This work was supported in part by Schweizerischer Nationalfonds.

APPENDIX A: WILSON COEFFICIENTS AT μ_W

We list here the functions introduced in the text, which define the Wilson coefficients at the matching scale [see Eqs. (16)–(18)].

1. SM case

The LO functions are ($x=m_t^2/M_w^2$)

$$C^0_{7,\rm SM}=\frac{x}{24}\left[\frac{-8x^3+3x^2+12x-7+(18x^2-12x)\ln x}{(x-1)^4}\right]$$

$$C^0_{8,\rm SM}=\frac{x}{8}\left[\frac{-x^3+6x^2-3x-2-6x\,\ln x}{(x-1)^4}\right]. \tag{A1}$$

In the $\overline{\rm MS}$ scheme, we have at the NLO

$$E_0=\frac{x(x^2+11x-18)}{12(x-1)^3}+\frac{x^2(4x^2-16x+15)}{6(x-1)^4}\ln x-\frac{2}{3}\ln x-\frac{2}{3},$$

$$W_{7,\mathrm{SM}}=\frac{-16x^4-122x^3+80x^2-8x}{9(x-1)^4}\mathrm{Li}_2\left(1-\frac{1}{x}\right)+\frac{6x^4+46x^3-28x^2}{3(x-1)^5}\ln^2 x$$
$$+\frac{-102x^5-588x^4-2262x^3+3244x^2-1364x+208}{81(x-1)^5}\ln x$$
$$+\frac{1646x^4+12\,205x^3-10\,740x^2+2509x-436}{486(x-1)^4},$$

$$W_{8,\mathrm{SM}}=\frac{-4x^4+40x^3+41x^2+x}{6(x-1)^4}\mathrm{Li}_2\left(1-\frac{1}{x}\right)+\frac{-17x^3-31x^2}{2(x-1)^5}\ln^2 x$$
$$+\frac{-210x^5+1086x^4+4893x^3+2857x^2-1994x+280}{216(x-1)^5}\ln x$$
$$+\frac{737x^4-14\,102x^3-28\,209x^2+610x-508}{1296(x-1)^4},$$

$$M_{7,\mathrm{SM}}=\frac{82x^5+301x^4+703x^3-2197x^2+1319x-208-(162x^4+1242x^3-756x^2)\ln x}{81(x-1)^5},$$

$$M_{8,\mathrm{SM}}=\frac{77x^5-475x^4-1111x^3+607x^2+1042x-140+(918x^3+1674x^2)\ln x}{108(x-1)^5},$$

$$T_{7,\mathrm{SM}}=\frac{x}{3}\left[\frac{47x^3-63x^2+9x+7-(18x^3+30x^2-24x)\ln x}{(x-1)^5}\right],$$

$$T_{8,\mathrm{SM}}=2x\left[\frac{-x^3-9x^2+9x+1+(6x^2+6x)\ln x}{(x-1)^5}\right]. \tag{A2}$$

2. 2HDM case, coupling $|Y|^2$

The functions relative to charged Higgs contributions, with coupling $|Y|^2$, are at the LO ($y=m_t^2/m_H^2$)

$$C^0_{7,YY}=\frac{1}{3}C^0_{7,\mathrm{SM}}(x\to y)$$

$$C^0_{8,YY}=\frac{1}{3}C^0_{8,\mathrm{SM}}(x\to y), \tag{A3}$$

at the NLO

$$E_H=\frac{1}{36}y\left[\frac{7y^3-36y^2+45y-16+(18y-12)\ln y}{(y-1)^4}\right],$$

$$W_{7,YY}=\frac{2}{9}y\left[\frac{8y^3-37y^2+18y}{(y-1)^4}\mathrm{Li}_2\left(1-\frac{1}{y}\right)+\frac{3y^3+23y^2-14y}{(y-1)^5}\ln^2 y+\frac{21y^4-192y^3-174y^2+251y-50}{9(y-1)^5}\ln y\right.$$
$$\left.+\frac{-1202y^3+7569y^2-5436y+797}{108(y-1)^4}\right]-\frac{4}{9}E_H,$$

$$W_{8,YY}=\frac{1}{6}y\left[\frac{13y^3-17y^2+30y}{(y-1)^4}\mathrm{Li}_2\left(1-\frac{1}{y}\right)-\frac{17y^2+31y}{(y-1)^5}\ln^2 y+\frac{42y^4+318y^3+1353y^2+817y-226}{36(y-1)^5}\ln y\right.$$

$$+\frac{-4451y^3+7650y^2-18\,153y+1130}{216(y-1)^4}\Bigg]-\frac{1}{6}E_H,$$

$$M_{7,YY}=\frac{1}{27}y\left[\frac{-14y^4+149y^3-153y^2-13y+31-(18y^3+138y^2-84y)\ln y}{(y-1)^5}\right],$$

$$M_{8,YY}=\frac{1}{36}y\left[\frac{-7y^4+25y^3-279y^2+223y+38+(102y^2+186y)\ln y}{(y-1)^5}\right],$$

$$T_{7,YY}=\frac{1}{3}T_{7,\mathrm{SM}}(x\to y),$$

$$T_{8,YY}=\frac{1}{3}T_{8,\mathrm{SM}}(x\to y). \tag{A4}$$

3. 2HDM case, coupling (XY^*)

Similarly, the functions relative to the charged Higgs contributions proportional to (XY^*) are at the LO

$$C^0_{7,XY}=\frac{1}{12}y\left[\frac{-5y^2+8y-3+(6y-4)\ln y}{(y-1)^3}\right],$$

$$C^0_{8,XY}=\frac{1}{4}y\left[\frac{-y^2+4y-3-2\ln y}{(y-1)^3}\right] \tag{A5}$$

and at the NLO

$$W_{7,XY}=\frac{4}{3}y\left[\frac{8y^2-28y+12}{3(y-1)^3}\mathrm{Li}_2\left(1-\frac{1}{y}\right)+\frac{3y^2+14y-8}{3(y-1)^4}\ln^2 y+\frac{4y^3-24y^2+2y+6}{3(y-1)^4}\ln y+\frac{-2y^2+13y-7}{(y-1)^3}\right],$$

$$W_{8,XY}=\frac{1}{3}y\left[\frac{17y^2-25y+36}{2(y-1)^3}\mathrm{Li}_2\left(1-\frac{1}{y}\right)-\frac{17y+19}{(y-1)^4}\ln^2 y+\frac{14y^3-12y^2+187y+3}{4(y-1)^4}\ln y-\frac{3(29y^2-44y+143)}{8(y-1)^3}\right],$$

$$M_{7,XY}=\frac{2}{9}y\left[\frac{-8y^3+55y^2-68y+21-(6y^2+28y-16)\ln y}{(y-1)^4}\right],$$

$$M_{8,XY}=\frac{1}{6}y\left[\frac{-7y^3+23y^2-97y+81+(34y+38)\ln y}{(y-1)^4}\right],$$

$$T_{7,XY}=\frac{2}{3}y\left[\frac{13y^2-20y+7-(6y^2+4y-4)\ln y}{(y-1)^4}\right],$$

$$T_{8,XY}=2y\left[\frac{-y^2-4y+5+(4y+2)\ln y}{(y-1)^4}\right]. \tag{A6}$$

APPENDIX B: ANOMALOUS DIMENSION MATRIX

For completeness, we give the anomalous dimension matrix which govern the evolution of the Wilson coefficients from μ_w to μ_b. It can be expanded perturbatively as

$$\gamma^{\mathrm{eff}}_{ji}(\mu)=\frac{\alpha_S(\mu)}{4\pi}\,\gamma^{0,\mathrm{eff}}_{ji}+\frac{\alpha_S^2(\mu)}{(4\pi)^2}\,\gamma^{1,\mathrm{eff}}_{ji}+\mathcal{O}(\alpha_S^3). \tag{B1}$$

The matrix $\gamma_{ji}^{0,\mathrm{eff}}$ is given by

$$\{\gamma_{ji}^{0,\mathrm{eff}}\}=\begin{bmatrix} -4 & \frac{8}{3} & 0 & -\frac{2}{9} & 0 & 0 & -\frac{208}{243} & \frac{173}{162} \\ 12 & 0 & 0 & \frac{4}{3} & 0 & 0 & \frac{416}{81} & \frac{70}{27} \\ 0 & 0 & 0 & -\frac{52}{3} & 0 & 2 & -\frac{176}{81} & \frac{14}{27} \\ 0 & 0 & -\frac{40}{9} & -\frac{100}{9} & \frac{4}{9} & \frac{5}{6} & -\frac{152}{243} & -\frac{587}{162} \\ 0 & 0 & 0 & -\frac{256}{3} & 0 & 20 & -\frac{6272}{81} & \frac{6596}{27} \\ 0 & 0 & -\frac{256}{9} & \frac{56}{9} & \frac{40}{9} & -\frac{2}{3} & \frac{4624}{243} & \frac{4772}{81} \\ 0 & 0 & 0 & 0 & 0 & 0 & \frac{32}{3} & 0 \\ 0 & 0 & 0 & 0 & 0 & 0 & -\frac{32}{9} & \frac{28}{3} \end{bmatrix} \tag{B2}$$

and in the $\overline{\mathrm{MS}}$ scheme with fully anticommuting γ_5, $\gamma_{ji}^{1,\mathrm{eff}}$ is [21]

$$\{\gamma_{ji}^{1,\mathrm{eff}}\}=\begin{bmatrix} -\frac{355}{9} & -\frac{502}{27} & -\frac{1412}{243} & -\frac{1369}{243} & \frac{134}{243} & -\frac{35}{162} & -\frac{818}{243} & \frac{3779}{324} \\ -\frac{35}{3} & -\frac{28}{3} & -\frac{416}{81} & \frac{1280}{81} & \frac{56}{81} & \frac{35}{27} & \frac{508}{81} & \frac{1841}{108} \\ 0 & 0 & -\frac{4468}{81} & -\frac{31\,469}{81} & \frac{400}{81} & \frac{3373}{108} & \frac{22\,348}{243} & \frac{10\,178}{81} \\ 0 & 0 & -\frac{8158}{243} & -\frac{59\,399}{243} & \frac{269}{486} & \frac{12\,899}{648} & -\frac{17\,584}{243} & -\frac{17\,2471}{648} \\ 0 & 0 & -\frac{251\,680}{81} & -\frac{128\,648}{81} & \frac{23\,836}{81} & \frac{6106}{27} & \frac{1\,183\,696}{729} & \frac{2\,901\,296}{243} \\ 0 & 0 & \frac{58\,640}{243} & -\frac{26\,348}{243} & -\frac{14\,324}{243} & -\frac{2551}{162} & \frac{2\,480\,344}{2187} & -\frac{3\,296\,257}{729} \\ 0 & 0 & 0 & 0 & 0 & 0 & \frac{4688}{27} & 0 \\ 0 & 0 & 0 & 0 & 0 & 0 & -\frac{2192}{81} & \frac{4063}{27} \end{bmatrix} \tag{B3}$$

APPENDIX C: ''RUNNING'' NUMBERS

The vectors $\{a_i\}$, $\{h_i\}$ and $\{a_i'\}$, $\{h_i'\}$ needed for the evaluation of the low-scale Wilson coefficients $C_7^{0,\mathrm{eff}}(\mu_b)$ and $C_8^{0,\mathrm{eff}}(\mu_b)$ are

$$\{a_i\}=\left\{\frac{14}{23},\frac{16}{23},\frac{6}{23},-\frac{12}{23},0.4086,-0.4230,-0.8994,0.1456\right\},$$

$$\{h_i\}=\left\{\frac{626\,126}{272\,277},-\frac{56\,281}{51\,730},-\frac{3}{7},-\frac{1}{14},\right.$$
$$\left.-0.6494,-0.0380,-0.0186,-0.0057\right\}, \tag{C1}$$

$$\{a_i'\}=\left\{\frac{14}{23},0.4086,-0.4230,-0.8994,0.1456\right\},$$

$$\{h_i'\}=\left\{\frac{313\,063}{363\,036},-0.9135,0.0873,-0.0571,0.0209\right\}; \tag{C2}$$

those needed for $C_7^{1,\mathrm{eff}}(\mu_b)$ are

$$\{e_i\}=\left\{\frac{46\,61\,194}{816\,831},-\frac{8516}{2217},0,0,-1.9043,-0.1008,0.1216,0.0183\right\},$$

$$\{f_i\}=\{-17.3023,8.5027,4.5508,0.7519,2.0040,0.7476,-0.5385,0.0914\},$$

$$\{k_i\}=\{9.9372,-7.4878,1.2688,-0.2925,-2.2923,-0.1461,0.1239,0.0812\},$$

$$\{l_i\}=\{0.5784,-0.3921,-0.1429,0.0476,-0.1275,0.0317,0.0078,-0.0031\}. \tag{C3}$$

APPENDIX D: VIRTUAL CORRECTION FUNCTIONS r_i

The renormalization scale-independent parts of the virtual corrections, encoded in the functions r_i in Eq. (30), read

$$r_1=-\frac{1}{6}\,r_2,$$

$$r_2=\frac{2}{243}\{-833+144\pi^2z^{3/2}+[1728-180\pi^2-1296\zeta(3)+(1296-324\pi^2)L+108L^2+36L^3]z$$
$$+[648+72\pi^2+(432-216\pi^2)L+36L^3]z^2+[-54-84\pi^2+1092L-756L^2]z^3\}$$
$$+\frac{16\pi i}{81}\{-5+[45-3\pi^2+9L+9L^2]z+[-3\pi^2+9L^2]z^2+[28-12L]z^3\}+\mathcal{O}(z^4),$$

$$r_7=\frac{32}{9}-\frac{8}{9}\,\pi^2,$$

$$r_8=-\frac{4}{27}\,(-33+2\pi^2-6i\pi), \tag{D1}$$

where z is defined as $z=m_c^2/m_b^2$ and the symbol L denotes $L=\ln(z)$. Notice that r_3, r_4, r_5, and r_6 are not used in the approximation $C_i^{0,\mathrm{eff}}(\mu_b)=0$ $(i=3,4,5,6)$ used for the matrix elements.

APPENDIX E: BREMSSTRAHLUNG f_{ij} TERMS

The expressions for the bremsstrahlung functions f_{ij} we use in the present paper are obtained after integrating one variable in the expressions given in Appendix B in Ref. [18]. The explicit expressions read (converted to the operator basis 12)

$$f_{11}=\frac{1}{36}\,f_{22},$$

TABLE I. Central value of our input parameters (first line) and their uncertainties (second line).

$\alpha_s(M_z)$	m_t (GeV)	m_c/m_b	m_b-m_c (GeV)	α_{em}^{-1}	$\lvert V_{ts}^{\star}V_{tb}/V_{cb}\rvert^2$	$B_{\rm SL}$
0.119	175	0.29	3.39	130.3	0.95	0.1049
± 0.004	± 5.0	± 0.02	± 0.04	± 2.3	± 0.03	± 0.0046

$$f_{12}=-\frac{1}{3}f_{22},$$

$$f_{17}=-\frac{1}{6}f_{27},$$

$$f_{18}=-\frac{1}{6}f_{28},$$

$$f_{22}=\frac{16z}{27}\int_0^{1/z}dt(1-zt)^2\left|\frac{G(t)}{t}+\frac{1}{2}\right|^2,$$

$$f_{27}=-\frac{8z^2}{9}\int_0^{1/z}dt(1-zt)\left(G(t)+\frac{t}{2}\right),$$

$$f_{28}=-\frac{1}{3}f_{27},$$

$$f_{78}=\frac{8}{9}\left(\frac{25}{12}-\frac{\pi^2}{6}\right),$$

$$f_{88}=\frac{1}{27}\left(\frac{16}{3}-\frac{4\pi^2}{3}+4\ln\frac{m_b}{\mu_b}\right), \tag{E1}$$

where z is $z=m_c^2/m_b^2$ and μ_b is the renormalization scale. The function $G(t)$ appearing in Eq. (E1) reads

$$G(t)=\begin{cases}-2\arctan^2\sqrt{\dfrac{t}{4-t}} & \text{for } t<4,\\ -\pi^2/2+2\ln^2\left(\dfrac{\sqrt{t}+\sqrt{t-4}}{2}\right)-2i\pi\ln\left(\dfrac{\sqrt{t}+\sqrt{t-4}}{2}\right) & \text{for } t\geqslant 4.\end{cases} \tag{E2}$$

APPENDIX F: INPUT PARAMETERS

We list in Table I the values of input parameters used in our calculation. The masses m_t, m_b, and m_c are understood to be the pole masses of the top, bottom, and charm quark. The value of the m_t is obtained by combining the results given in Refs. [50, 51]; those of the two combinations of m_c and m_b are taken from Ref. [24]. For α_{em} and $\lvert V_{ts}^{*}V_{tb}/V_{cb}\rvert^2$ we refer to Refs. [52] and [53], respectively. We take $\alpha_S(M_Z)=0.119\pm 0.004$, as an average between a pessimistic and optimistic estimate of the error [54], as suggested in Ref. [55]. The value of the semileptonic branching ratio $B_{\rm SL}$ has been recently obtained by the CLEO Collaboration [56]. The other constants used in the calculation are $M_W=80.33$ GeV, $\lambda_1=-0.5$ GeV^2, and $\lambda_2=0.12$ GeV^2.

[1] S. Bertolini, F. Borzumati, and A. Masiero, in *B Decays*, edited by S. Stone (World Scientific, Singapore, 1992), pp. 458–478; *ibid.*, 2nd ed. pp. 620–643.

[2] J. L. Hewett, Phys. Rev. Lett. **70**, 1045 (1993); V. Barger, M. Berger, and R. J. N. Phillips, *ibid.* **70**, 1368 (1993).

[3] S. Dimopoulos and H. Georgi, Nucl. Phys. **B193**, 150 (1981).

[4] For a discussion within the minimal supersymmetric standard model see F. Borzumati, Z. Phys. C **63**, 291 (1994); F. Borzumati and N. Polonsky, Contribution to e^+e^- Collisions at TeV Energies: The Physics Potential, Annecy, Gran Sasso, Hamburg, 1995, edited by P. M. Zerwas, hep-ph/9602433.
[5] CLEO Collaboration, M. S. Alam *et al.*, Phys. Rev. Lett. **74**, 2885 (1995).
[6] ALEPH Collaboration, R. Barate *et al.*, Report No. CERN-EP/98-044.
[7] S. Bertolini, F. Borzumati, and A. Masiero, Phys. Rev. Lett. **59**, 180 (1987); N. G. Deshpande, P. Lo, J. Trampetic, G. Eilam, and P. Singer, *ibid.* **59**, 183 (1987).
[8] B. Grinstein, R. Springer, and M. B. Wise, Phys. Lett. B **202**, 138 (1988); Nucl. Phys. **B339**, 269 (1990).
[9] K. Adel and Y. P. Yao, Mod. Phys. Lett. A **8**, 1679 (1993); M. Ciuchini, E. Franco, G. Martinelli, L Reina, and L. Silverstrini, Phys. Lett. B **316**, 127 (1993); M. Ciuchini, E. Franco, L. Reina, and L. Silvestrini, Nucl. Phys. **B421**, 41 (1994); M. Ciuchini, E. Franco, G. Martinelli, and L. Reina, Phys. Lett. B **301**, 263 (1993); Nucl. Phys. **B415**, 403 (1994); M. Misiak, *ibid.* **B393**, 23 (1993); **B439**, 461(E) (1995); G. Cella, G. Curci, G. Ricciardi, and A. Viceré, Phys. Lett. B **325**, 227 (1994); Nucl. Phys. **B431**, 417 (1994).
[10] A. Ali and C. Greub, Z. Phys. C **49**, 431 (1991); Phys. Lett. B **259**, 182 (1991); **361**, 146 (1995).
[11] A. Ali and C. Greub, Z. Phys. C **60**, 433 (1993).
[12] M. Ciuchini, E. Franco, G. Martinelli, L. Reina, and L. Silvestrini, Phys. Lett. B **334**, 137 (1994).
[13] A. J. Buras, M. Misiak, M. Münz, and S. Pokorski, Nucl. Phys. **B424**, 374 (1994).
[14] K. Adel and Y. P. Yao, Phys. Rev. D **49**, 4945 (1994).
[15] C. Greub and T. Hurth, Phys. Rev. D **56**, 2934 (1997).
[16] A. J. Buras, A. Kwiatkowski, and N. Pott, Nucl. Phys. **B517**, 353 (1998).
[17] M. Ciuchini, G. Degrassi, P. Gambino, and G. F. Giudice, hep-ph/9710335.
[18] C. Greub, T. Hurth, and D. Wyler, Phys. Lett. B **380**, 385 (1996); Phys. Rev. D **54**, 3350 (1996).
[19] A. J. Buras, M. Jamin, M. E. Lautenbacher, and P. H. Weisz, Nucl. Phys. **B370**, 69 (1992); **B375**, 501 (1992).
[20] M. Misiak and M. Münz, Phys. Lett. B **344**, 308 (1995).
[21] K. Chetyrkin, M. Misiak, and M. Münz, Phys. Lett. B **400**, 206 (1997).
[22] K. Chetyrkin, M. Misiak, and M. Münz, Nucl. Phys. **B518**, 473 (1998).
[23] A. Falk, M. Luke, and M. Savage, Phys. Rev. D **49**, 3367 (1994).
[24] I. I. Bigi, M. Shifman, N. G. Uraltsev, and A. I. Vainshtein, Phys. Rev. Lett. **71**, 496 (1993).
[25] A. V. Manohar and M. B. Wise, Phys. Rev. D **49**, 1310 (1994); A. Falk, M. Luke, and M. Savage, *ibid.* **53**, 2491 (1996).
[26] M. B. Voloshin, Phys. Lett. B **397**, 275 (1997); Z. Ligeti, L. Randall, and M. B. Wise, *ibid.* **402**, 178 (1997); A. K. Grant, A. G. Morgan, S. Nussinov, and R. D. Peccei, Phys. Rev. D **56**, 3151 (1997); G. Buchalla, G. Isidori, and S. J. Rey, Nucl. Phys. **B511**, 594 (1998).
[27] A. J. Buras, A. Kwiatkowski, and N. Pott, Phys. Lett. B **414**, 157 (1997).
[28] W. S. Hou and R. S. Willey, Phys. Lett. B **202**, 591 (1988).
[29] V. Barger, J. L. Hewett, and R. J. N. Phillips, Phys. Rev. D **41**, 3421 (1990).
[30] S. Bertolini, F. Borzumati, A. Masiero, and G. Ridolfi, Nucl. Phys. **B353**, 591 (1991).
[31] P. Krawczyk and S. Pokorski, Nucl. Phys. **B364**, 11 (1991).
[32] Y. Grossman and Y. Nir, Phys. Lett. B **313**, 126 (1993); Y. Grossman, Y. Nir, and R. Rattazzi, hep-ph/9701231.
[33] P. Ciafaloni, A. Romanino, and A. Strumia, hep-ph/9710312.
[34] S. L. Glashow and S. Weinberg, Phys. Rev. D **15**, 1958 (1977).
[35] S. Weinberg, Phys. Rev. Lett. **37**, 657 (1976).
[36] C. H. Albright, J. Smith, and S.-H. H. Tye, Phys. Rev. D **21**, 711 (1980).
[37] G. C. Branco, A. J. Buras, and J. M. Gerard, Nucl. Phys. **B259**, 306 (1985).
[38] S. Weinberg, Phys. Rev. D **42**, 860 (1990).
[39] L. Lavoura, Int. J. Mod. Phys. A **8**, 375 (1993).
[40] H. E. Haber, G. L. Kane, and T. Sterling, Nucl. Phys. **B161**, 493 (1979).
[41] H. D. Politzer, Nucl. Phys. **B172**, 349 (1980); H. Simma, Z. Phys. C **61**, 67 (1994).
[42] T. Inami and C. S. Lim, Prog. Theor. Phys. **65**, 297 (1981).
[43] G. Buchalla, A. J. Buras, and M. Lautenbacher, Rev. Mod. Phys. **68**, 1125 (1996).
[44] N. Pott, Phys. Rev. D **54**, 938 (1996).
[45] N. Cabibbo and L. Maiani, Phys. Lett. **79B**, 109 (1978); C. S. Kim and A. D. Martin, Phys. Lett. B **225**, 186 (1989); Y. Nir, *ibid.* **221**, 184 (1989).
[46] C. Greub and T. Hurth, hep-ph/9708214.
[47] F. M. Borzumati and A. Djouadi (in preparation).
[48] A. Ali, Asatrian, and C. Greub, hep-ph/9803314.
[49] F. M. Borzumati, hep-ph/9702307.
[50] CDF Collaboration, S. Leone spokesperson, Proceedings of the High-energy Physics International Euroconference on Quantum Chromodynamics: QCD 97, Montpellier, France, 1997 (unpublished).
[51] D0 Collaboration, K. Genser spokesperson, Proceedings of the 11th Les Rencontres de Physique de la Vallee d'Aoste: Results and Perspectives in Particle Physics, La Thuile, Italy, 1997 (unpublished).
[52] S. Eidelman and F. Jegerlehner, Z. Phys. C **67**, 585 (1995).
[53] Particle Data Group, R. M. Barnett *et al.*, Phys. Rev. D **54**, 1 (1996).
[54] S. Bethke, talk given at High-energy Physics International Euroconference on Quantum Chromodynamics: QCD 97 [50], hep-ph/9710030.
[55] G. Altarelli, talk given at the XVIII International Symposium on Lepton-photon Interactions, Hamburg, 1997, hep-ph/9710434.
[56] CLEO Collaboration, B. Barish *et al.*, Phys. Rev. Lett. **76**, 1570 (1996).